J. Math. Study
doi: 10.4208/jms.v50n2.17.01

Vol. **50**, No. 2, pp. 101-143
June 2017

A Review of Prolate Spheroidal Wave Functions from the Perspective of Spectral Methods

Li-Lian Wang*

Division of Mathematical Sciences, School of Physical and Mathematical Sciences, Nanyang Technological University, 637371, Singapore.

Received 3 January, 2017; Accepted 29 March, 2017

Abstract. This paper is devoted to a review of the prolate spheroidal wave functions (PSWFs) and their variants from the viewpoint of spectral/spectral-element approximations using such functions as basis functions. We demonstrate the pros and cons over their polynomial counterparts, and put the emphasis on the construction of essential building blocks for efficient spectral algorithms.

AMS subject classifications: 33C47, 33E30, 41A30, 42C05, 65D32, 65N35

Key words: Prolate spheroidal wave functions and their generalisations, time-frequency concentration problem, bandlimited functions, finite Fourier/Hankel transforms, quasi-uniform grids, well-conditioned prolate collocation scheme, prolate-Galerkin method, spectral accuracy.

Contents

1 Introduction 102
2 Prolate spheroidal wave functions 105
2.1 Bandlimited functions . . . 105
2.2 Sturm-Liouville equation . . . 108
2.3 Analytic and asymptotic properties . . . 109
3 Numerics of PSWFs and prolate-differentiation schemes 110
3.1 Evaluation of PSWFs and the associated eigenvalues . . . 110
3.2 Kong-Rokhlin's rule . . . 112
3.3 Prolate points and prolate quadrature . . . 113
3.4 Prolate interpolation, cardinal basis and pseudospectral differentiation . . . 115
3.5 "Inverse" of prolate pseudospectral differentiation matrix . . . 116
3.6 Kong-Rokhlin's prolate-spectral differentiation schemes . . . 120
3.7 Novel differentiation schemes based on generalised PSWFs . . . 121

*Corresponding author. *Email address:* lilian@ntu.edu.sg (L.-L. Wang)

4 Spectral approximation results 124
4.1 c-bandlimited functions 125
4.2 Approximation results in Sobolev spaces 125
5 Prolate spectral/spectral-element methods 127
5.1 Prolate-pseudospectral/collocation methods for hyperbolic PDEs 127
5.2 Prolate-pseudospectral/collocation methods for BVPs 128
5.3 Prolate-collocation/Galerkin methods for eigenvalue problems 130
5.4 Prolate-element methods and nonconvergence of h-refinement 131
6 Generalisations of prolate spheroidal wave functions 134
6.1 Prolate spheroidal wave equation and generalised PSWFs 135
6.2 Oblate spheroidal wave functions 137
7 Concluding remarks 138

- *" Investigation of the problem of simultaneously concentrating a function and its Fourier transform differed from the other problems I have worked on in two fundamental ways. First, we solved it—completely, easily and quickly. Second, the answer was interesting—even elegant and beautiful."* — Slepian [85] (1983).

- *" The prolate spheroidal wave functions are likely to be a better tool for the design of spectral and pseudo-spectral techniques than the orthogonal polynomials and related functions."* — Xiao, Rokhlin and Yarvin [101] (2001).

- *" The prolate functions are the basis that is "plug-and-play" compatible with finite element or spectral element or other programs that employ Legendre polynomials. The claimed advantage of prolate functions is that they resolve wavy, bandlimited signals with only two points per wavelength, whereas Legendre polynomials and Chebyshev polynomials require a minimum of π degrees of freedom per wavelength."* — Boyd [9] (2013).

1 Introduction

Claude E. Shannon (1916–2001) once posed the question: *To what extent are functions, which are confined to a finite bandwidth, also concentrated in the time domain?* (cf. [60]). This open question was answered by David Slepian (1923-2007) *et al.* at Bell Laboratories in a series of seminal papers dated back to 1960s (see e.g., [53, 83, 86]). *" We found a second-order differential equation that commuted with an integral operator that was at the heart of the problem,"* as commented by D. Slepian in [85]. This statement best testifies to their findings: the prolate spheroidal wave functions of order zero (PSWFs), being the eigenfunctions of a second-order singular Sturm-Liouville equation, are coincidentally the spectrum of an integral operator related to the finite Fourier transform. It is also from the latter that a collection of remarkable properties of PSWFs was discovered. For example, PSWFs are bi-orthogonal in the sense that they are orthogonal over both a given finite interval and

the whole line $(-\infty,\infty)$; PSWFs are bandlimited functions; they are maximally concentrated within a finite time interval, and among others. Attributed to the contribution of D. Slepian, PSWFs are also termed as *Slepian functions* or *Slepian basis*.

There have been limited studies and applications of PSWFs over the first two decades after the seminal works of Slepian *et al.* *""Prolate Revivial" is by Xiao, Rokhlin and Yarvin [101]; recent articles include [41, 47, 107],"* as remarked by Boyd in the Book Review [9, P. 575] for Hogan and Lakey [36]. The recent monograph by Osipov, Rokhlin and Xiao [66] provided a comprehensive exposition of analytic, asymptotic properties, and numerics of PSWFs of order zero. It was meant to be in the spirit of classical texts such as *A Treatise on the Theory of Bessel Functions* by G. Watson [97]. As stated in the Preface, this book however touched very briefly on the wide-ranging applications of PSWFs. The book [36] targeted at the applications of PSWFs in sampling and signal processing, together with an accessible introduction to the mathematical theory related to PSWFs. However, it is far and away the best and most comprehensive review of modern numerical applications of prolate expansions (cf. [9]). Boyd *et al.* tabulated and highlighted in [10] more than thirty selected recent works on PSWFs.

In general, the research on PSWFs can be clarified into the following categories:

(i) Study of their analytic and asymptotic properties, numerical evaluations, prolate quadrature, interpolation and related issues (see, e.g., [4, 6, 8, 25, 37, 40, 43, 60, 66, 70, 73, 91, 99–101]);

(ii) Generalization of the Slepian's time-frequency concentration problem on a finite interval to other geometries, or introduction of generalized PSWFs in different senses (see, e.g., [20, 21, 30, 41, 42, 49, 59, 62, 68, 69, 81–83, 88, 94, 103]);

(iii) Development of numerical methods using PSWFs as basis functions, e.g., spectral/spectral-elements methods (see, e.g., [5, 7, 10, 13, 50, 51, 92, 107]), and wavelets (see, e.g., [15, 88–90]).

(iv) Diverse applications in sampling, signal processing, time series analysis and image processing (see, e.g., [12, 17, 26, 27, 35, 38, 46, 57, 74]).

This paper is devoted to a review of the PSWFs from the perspective of spectral and spectral-element methods. As the eigenfunctions of a singular Sturm-Liouville problem, the PSWFs are born with the orthogonality and completeness in L^2-space as with their counterparts–Legendre polynomials, so they can be a candidate for a basis of spectral algorithms. Then a natural question to ask is *why should the PSWF-based method be the method of choice in place of the polynomial-based counterpart (perhaps for certain problems)?* We hope to provide an answer to this question in what follows.

Firstly, the essence of Slepian's findings resides in that the PSWFs are simultaneously eigenfunctions of an integral operator related to the finite Fourier transform. As a result, they form an orthogonal basis of the Paley-Wiener space of c-bandlimited functions, and serve as *an optimal basis for approximating bandlimited functions*.

Secondly, PSWFs, as a generalization of Legendre polynomials, oscillate more uniformly than Legendre polynomials and any other Jacobi polynomials, as the bandwidth parameter c increases in a range. Thus, a better resolution can be achieved for approximation by PSWFs. Indeed, the study in e.g., [7] shows that the PSWFs only require two points per wavelength to resolve wavy, bandlimited signals, whereas Legendre polynomials and Chebyshev polynomials require a minimum of π points. The nearly uniform oscillations of PSWFs can relax the constraints of explicit time-discretization coupled with spatial approximations by spectral/spectral-element methods. However, the spectral grids are non-uniform and denser near the boundaries, which therefore suffer from a much severer constraint related to the Courant-Friedrichs-Lewy (CFL) condition than the uniform-grid-based methods. To overcome this difficulty, one might resort to semi-implicit and fully implicit time-discretization schemes, but they require robust solvers for the resultant systems when the scale is large. It is worthwhile to point out that Kosloff and Tal-Ezer [48] proposed a mapped spectral method to obtain an $O(N^{-1})$-CFL contraint Runge-Kutta method for first-order problems. However, the error analysis in [78] indicates that the accuracy is deteriorated for the suggested parameter in [48]. The prolate points are quasi-uniformly distributed. Shifting the points and basis from Legendre to PSWF can be accomplished in a compatible "plug-and-play" manner (cf. [8]). Chen, Gottlieb and Hesthaven [13] studied the prolate-pseudospectral method for first-order equations, and a relaxation of the CFL condition from $O(N^{-2})$ for the Legendre and Chebyshev spectral methods to $O(N^{-3/2})$ for PSWFs was observed with suitable choice of the bandwidth parameter c. A similar gain in prolate-elements for advection problems on the sphere was found in [107].

A critical issue in using PSWFs as basis functions is the choice of bandwidth parameter c. A rule of thumb is that one should choose $c=c(N)$ to achieve better uniformity of grid distribution without loss of spectral accuracy. Note that for $c\gg N$, the PSWFs behave like Hermite functions (cf. [7, (17)]), so they decay to zero in the neighbourhoods of the endpoints $x=\pm 1$. In this case, the PSWFs lose the approximability to general functions on $(-1,1)$. A "transition bandwidth" derived from asymptotic formulas of PSWFs (cf. [58, 84]): $c_*(N)=\pi(N+1/2)/2$ was recommended by [7], where the feasible range of c should be $0<c<c_*(N)$. However, both numerical evidences and analysis indicate that the choice of c close to $c_*(N)$ degrades the accuracy. A more reliable upper bound was derived in Wang and Zhang [95] (see Theorem 4.3). From a different perspective, Kong and Rokhlin [47] proposed a useful rule for pairing up (c,N). The essential idea is that given the bandwidth parameter c, one chooses N such that the prolate quadrature rule is exact for complex exponentials and bandlimited functions to a prescribed accuracy. Such a rule appears more reasonable as the PSWFs can best approximate the class of c-bandlimited functions. We remark that a more practice route to implement this rule can be found in [96].

It is beneficial to employ PSWF-spectral/spectral-element methods, when the underlying solution is wavy or almost bandlimited. However, PSWFs are anyhow a non-polynomial basis, and might lose certain capabilities of polynomials, when they are used

for solving PDEs. For example, they exhibit the nonconvergence of h-refinement in prolate-element methods, which was first pointed out by Boyd *et al.* [10] by simply examining hp-prolate approximation of the trivial function $u(x)=1$. Indeed, PSWFs also lack some properties of polynomials which are important for efficient spectral algorithms. Therefore, a naive extension of existing algorithms to this setting might be unsatisfactory or fail to work at times, so the related numerical issues are worthy of investigation.

The purpose of this paper is to review the state-of-the-art in spectral and spectral-element methods using PSWFs as basis functions. As outlined in Contents, with some introduction of the background and properties of PSWFs, we then focus on the building blocks for spectral algorithms, and on the related spectral approximations results, and applications of prolate spectral/spectral-element methods. We conclude the paper with several relevant generalisations of PSWFs.

2 Prolate spheroidal wave functions

In this section, we briefly review the two contexts, from which the PSWFs of order zero arise, and collect some important properties of PSWFs (cf. [36, 66, 83, 85, 86, 101]).

2.1 Bandlimited functions

Let $L^2(\mathbb{R})$ be the space of square integrable functions on the whole line $\mathbb{R}:=(-\infty,\infty)$. For any function $f(t)\in L^2(\mathbb{R})$, we have the Fourier transform and inverse Fourier transform:

$$\mathscr{F}(\omega)=\int_{-\infty}^{\infty} f(t)e^{-\mathrm{i}\omega t}dt;\quad f(t)=\frac{1}{2\pi}\int_{-\infty}^{\infty}\mathscr{F}(\omega)e^{\mathrm{i}\omega t}d\omega. \tag{2.1}$$

There holds the Parseval's identity:

$$\int_{-\infty}^{\infty} f(t)g^*(t)dt=\frac{1}{2\pi}\int_{-\infty}^{\infty}\mathscr{F}(\omega)\mathscr{G}^*(\omega)d\omega, \tag{2.2}$$

where the notation " * " stands for the complex conjugate.

We are interested in a subclass of functions $f(t)\in L^2(\mathbb{R})$, whose Fourier transform $\mathscr{F}(\omega)$ vanishes if $|\omega|>W$ for some *bandwidth parameter* $W>0$. Such a function f is called *W-bandlimited*. The space of all W-bandlimited functions is known as the Paley-Wiener space, defined by

$$\mathcal{B}_W=\big\{f\in L^2(\mathbb{R}):\mathrm{supp}\big(\mathscr{F}(\omega)\big)\subset[-W,W]\big\}. \tag{2.3}$$

As an essential characterisation of a W-bandlimited function, the Paley-Wiener theorem [67] states that *f is W-bandlimited, if and only if*

$$f(t)=\int_{-W}^{W} e^{-\mathrm{i}\omega t}g(\omega)d\omega,\quad \textit{for some}\ \ g\in L^2(-W,W), \tag{2.4}$$

DOI https://doi.org/10.4208/jms.v50n2.17.01 | Generated on 2024-11-19 16:37:05

and if and only if f is an entire function in $L^2(\mathbb{R})$ and of exponential type, i.e.,

$$|f(z)|\leq \sup_{x\in\mathbb{R}}|f(x)|\, e^{W|y|},\quad z=x+\mathrm{i}y.$$

A fundamental sampling theorem says that (see, e.g., [102]): *if $f\in\mathcal{B}_W$, then it can be completely reconstructed from the sample $\{f(j\pi/W)\}_{j\in\mathbb{Z}}$ (where $\mathbb{Z}$ is the set of all integers), namely,*

$$f(t)=\sum_{j\in\mathbb{Z}}\frac{\sin W(t-t_j)}{W(t-t_j)}f(t_j),\quad t_j=\frac{j\pi}{W}.$$

It is known that any nontrivial signal cannot be simultaneously bandlimited and time-limited, that is, a function and its Fourier transform cannot both have finite support. Then a natural question to ask is: *Given a fixed interval, say, $(-T/2,T/2)$, to what extent that the energy of $f(t)\in\mathcal{B}_W$ can be concentrated on this interval?* This is basically the *time-frequency concentration problem* that attracted much attention of D. Slepian *et al.* in 1960s [85]. The problem of interest was actually boiled down to the study of the Fredholm integral equation of the second kind: find $\mu\in\mathbb{R}$ and ψ such that

$$\mathcal{Q}_c[\psi](x):=\int_{-1}^{1}\frac{\mathrm{sinc}(x-t)}{\pi(x-t)}\psi(t)\,dt=\mu\psi(x),\quad c>0, \tag{2.5}$$

where x is in the reference interval $\Lambda:=(-1,1)$, and $c=\pi WT$ is also called the bandwidth parameter. Using the fundamental identity:

$$\sigma_c(t):=\frac{\mathrm{sinc}t}{\pi t}=\frac{c}{2\pi}\int_{-1}^{1}e^{\mathrm{i}c\omega t}d\omega, \tag{2.6}$$

one verifies readily that

$$\mathcal{Q}_c[\phi](x)=\frac{2\pi}{c}\big(\mathcal{F}_c^*\circ\mathcal{F}_c\big)[\phi](x), \tag{2.7}$$

where

$$\mathcal{F}_c[\phi](x):=\int_{-1}^{1}e^{\mathrm{i}cxt}\phi(t)\,dt,\quad \mathcal{F}_c^*[\phi](x):=\int_{-1}^{1}e^{-\mathrm{i}cxt}\phi(t)\,dt. \tag{2.8}$$

Remark 2.1. We see from (2.6) that the Fourier transform of $\sigma_c(t)$ is $c\cdot\chi_{[-1,1]}(\omega)$ (where $\chi_{[-1,1]}(\omega)$ is the indicate function of the interval $[-1,1]$), so σ is 1-bandlimited. Noting that $\sigma_c(t)$ is an even function, we find from (2.6) that the Fourier transform (in t) of $\sigma_c(x-t)(=\sigma_c(t-x))$ is $c\cdot e^{-\mathrm{i}x\omega}\chi_{[-1,1]}(\omega)$. Thus, by the Parseval's identity (2.2) and (2.6),

$$\int_{-\infty}^{\infty}\frac{\mathrm{sinc}(x-t)}{\pi(x-t)}\cdot\frac{\mathrm{sinc}(t-y)}{\pi(t-y)}\,dt=c\cdot\frac{\mathrm{sinc}(x-y)}{\pi(x-y)}. \tag{2.9}$$

It is a very useful identity for the derivation of the orthogonality (2.16) below.

Based on the standard spectral theory (cf. [14]), the operator $\mathcal{Q}_c$ has a countable set of spectrum and eigenfunctions $\{(\mu_n,\psi_n)\}_{n=0}^{\infty}$, namely,

$$\int_{-1}^{1}\frac{\sin c(x-t)}{\pi(x-t)}\psi_n(t;c)\,dt=\mu_n(c)\,\psi_n(x;c),\quad n\geq 0,\ \ c>0, \tag{2.10}$$

with the properties:

(i) all the eigenvalues are distinct, real and positive, and can be ordered as

$$\mu_0(c)>\mu_1(c)>\cdots>\mu_n(c)>\cdots>0\quad(\text{note: }\lim_{n\to\infty}\mu_n(c)=0); \tag{2.11}$$

(ii) the corresponding eigenfunctions $\{\psi_n\}_{n=0}^{\infty}$ are orthogonal and complete in $L^2(\Lambda)$, which are conventionally normalized as

$$\int_{-1}^{1}\psi_n(x;c)\psi_m(x;c)\,dx=\delta_{mn}=\begin{cases}0, & \text{if } m\neq n,\\ 1, & \text{if } m=n.\end{cases} \tag{2.12}$$

The function $\psi_n(x;c)$ is termed as *the PSWF of degree n with bandwidth c*.

The relation (2.7) implies that $\mathcal{Q}_c$ and $\mathcal{F}_c$ share the same eigenfunctions $\{\psi_n\}_{n=0}^{\infty}$:

$$\mathrm{i}^n\lambda_n(c)\psi_n(x;c)=\int_{-1}^{1}e^{\mathrm{i}cxt}\psi_n(t;c)\,dt,\quad n\geq 0, \tag{2.13}$$

where the corresponding eigenvalues $\{\lambda_n(c)\}$ (modulo the factor i^n) are all real, positive and simple. Moreover, we have the relation:

$$\mu_n(c)=\frac{c}{2\pi}\lambda_n^2(c)\quad\text{or}\quad\lambda_n(c)=\sqrt{\frac{2\pi}{c}\mu_n(c)}\,, \tag{2.14}$$

so by (2.11), $\{\lambda_n(c)\}$ are in descending order and $\lambda_n(c)\to 0$ as $n\to\infty$.

Remark 2.2. One verifies from (2.13) and the parity (see (2.28) below) that

$$\psi_n(x;c)=\frac{\mathrm{i}^n}{c\lambda_n(c)}\int_{-c}^{c}\psi_n\Big(\frac{\omega}{c};c\Big)e^{-\mathrm{i}\omega x}d\omega, \tag{2.15}$$

so by (2.4), the PSWF $\psi_n(x;c)$ is c-bandlimited.

Remark 2.3. Observe from (2.10) and (2.13) that $\{\psi_n(x;c)\}$ are well-defined for all $x\in\mathbb{R}$. Surprisingly, they are also mutually orthogonal on $\mathbb{R}$:

$$\int_{-\infty}^{\infty}\psi_n(x;c)\psi_m(x;c)\,dx=\frac{1}{\mu_n(c)}\delta_{mn}, \tag{2.16}$$

which follows from (2.9)-(2.10) (see [86]).

Remark 2.4. An analogue of (2.13) for the Fourier transform is associated with the Hermite functions (cf. [18, P. 22]):

$$\int_{-\infty}^{\infty} \mathcal{H}_n(t)e^{-\mathrm{i}\omega t}dt = (-\mathrm{i})^n\sqrt{2\pi}\mathcal{H}_n(\omega),\ \ n=0,1,\cdots, \tag{2.17}$$

where $\mathcal{H}_n(t)$ is the Hermite function defined by the Hermite polynomial $H_n(t)$ of degree n as follows:

$$\mathcal{H}_n(t) = (2^n n!\sqrt{\pi})^{-1/2}e^{-t^2/2}H_n(t), \quad H_n(t) = (-1)^n e^{t^2}\frac{d^n}{dt^n}\{e^{-t^2}\}. \tag{2.18}$$

This analytic tool played an important part in developing efficient spectral methods for scattering problems with unbounded rough scattering surfaces [33]. It is also noteworthy that Li [54] used (2.17) with $\omega=\mathrm{i}a$ (for any complex number a) in the convergence analysis of the Hermite expansion of the Riemann Zeta function.

Hereafter, we shall not always specify the dependence of the notation on the bandwidth parameter c, whenever it is clear from the context.

2.2 Sturm-Liouville equation

One significant discovery of D. Slepian *et al.* is that the integral operators in (2.8) are commutable with the second-order differential operator:

$$\mathcal{D}_x^c = -\frac{d}{dx}(1-x^2)\frac{d}{dx} + c^2x^2, \tag{2.19}$$

in the sense that

$$\mathcal{D}_x^c\int_{-1}^{1}\frac{\sin c(x-t)}{\pi(x-t)}\psi_n(t)dt = \int_{-1}^{1}\frac{\sin c(x-t)}{\pi(x-t)}\mathcal{D}_t^c\psi_n(t)dt. \tag{2.20}$$

Thus $\{\psi_n\}$ are also eigenfunctions of the singular Sturm-Liouville problem:

$$\mathcal{D}_x^c\psi_n(x) = \chi_n\psi_n(x), \quad x\in\Lambda=(-1,1),\ \ n\geq 0, \tag{2.21}$$

where $\{\chi_n\}$ are the corresponding eigenvalues such that

$$0<\chi_0<\chi_1<\cdots<\chi_n<\cdots; \quad \lim_{n\to\infty}\chi_n=\infty. \tag{2.22}$$

The eigen-problem (2.21) arises from solving the Helmholtz equation in prolate spheroidal coordinates by separation of variables. It is a special case of the spheroidal wave equation (see (6.2) below) with $m=0$, so we call the eigenfunctions PSWFs *of order zero*.

Recall that the Legendre polynomials $\{P_n(x)\}$ satisfy

$$\mathcal{D}_x^0P_n(x) = -\big((1-x^2)P_n'(x)\big)' = n(n+1)P_n(x), \tag{2.23}$$

and the three-term recurrence relation (cf. [87]):

$$\begin{aligned}&(n+1)P_{n+1}(x)=(2n+1)xP_n(x)-nP_{n-1}(x),\quad n\geq 1,\\&P_0(x)=1,\quad P_1(x)=x.\end{aligned}\tag{2.24}$$

We also use the orthonormal Legendre polynomials defined by

$$\overline{P}_n(x)=\sqrt{n+\frac{1}{2}}\,P_n(x),\quad \text{so}\quad \int_{-1}^{1}\overline{P}_n(x)\overline{P}_m(x)dx=\delta_{mn}.\tag{2.25}$$

We see that PSWFs are generalization of Legendre polynomials, as

$$\psi_n(x;0)=\overline{P}_n(x),\quad \chi_n(0)=n(n+1).\tag{2.26}$$

Remark 2.5. The integral equation (2.13) does not hold when $c=0$. In other words, the Legendre polynomials are not bandlimited, which can also be seen from the formula (see [22, P. 213]):

$$\int_{-1}^{1}P_n(\omega)e^{-\mathrm{i}\omega x}d\omega=(-\mathrm{i})^n(2n+1)\sqrt{\frac{\pi}{2}}\frac{J_{n+1/2}(x)}{\sqrt{x}},\tag{2.27}$$

where the Bessel function $J_{n+1/2}(\cdot)$ is not compactly supported. On the other hand, we have from (2.4) that the Fourier transform of $J_{n+1/2}(x)/\sqrt{x}$ is $P_n(x)$ up to a constant multiple, so it is bandlimited. Since a function and its Fourier transform can not both have a finite support, $P_n(x)$ is not bandlimited, as opposite to the PSWF (see (2.15)).

2.3 Analytic and asymptotic properties

We collect some relevant properties of PSWFs, and refer to [66] for many others.

- We have the parity
$$\psi_n(-x;c)=(-1)^n\psi_n(x;c),\tag{2.28}$$
so $\psi_n(x;c)$ with even n is even in x, but it is an odd function when n is odd.
- The PSWF $\psi_n(x;c)$ has exactly n real distinct zeros in the interval $(-1,1)$. However, unlike the Legendre polynomial, it also has infinitely many real zeros outside $(-1,1)$ (cf. [66]).
- For fixed $c>0$ and large n, we have
$$\psi_n(x;c)=\overline{P}_n(x)+\frac{c^2}{16n}\big(\overline{P}_{n-2}(x)-\overline{P}_{n+2}(x)\big)+O\Big(\frac{c^2}{n^2}\Big).\tag{2.29}$$
For large c and fixed n, PSWFs behave like scaled Hermite functions:
$$\psi_n(x;c)\sim e^{-cx^2/2}H_n(\sqrt{c}x).\tag{2.30}$$

- We have the uniform bounds:

$$n(n+1)<\chi_n(c)<n(n+1)+c^2,\quad n\geq 0,\ c>0. \tag{2.31}$$

For fixed c and large n, we have (see [70, (64)]):

$$\chi_n(c)=n(n+1)+\frac{c^2}{2}+\frac{c^2(4+c^2)}{32n^2}\Big(1-\frac{1}{n}+O(n^{-2})\Big),\quad \forall n\gg 1. \tag{2.32}$$

For fixed n and large c, $\chi_n(c)$ behaves like (see [100, (1.1)]):

$$\chi_n(c)=c(2n+1)-\frac{n^2+n+3/2}{2}+O(c^{-1}),\quad \forall c\gg 1. \tag{2.33}$$

- We have the representation for $\lambda_n(c)$ in terms of $\psi_n(1;c)$ (see [70, Thm. 9]):

$$\lambda_n(c)=\frac{\sqrt{\pi}c^n(n!)^2}{(2n)!\Gamma(n+3/2)}\cdot\exp\Big(\int_0^c\Big(\frac{2(\psi_n(1;\tau))^2-1}{2\tau}-\frac{n}{\tau}\Big)d\tau\Big),\quad \forall c>0. \tag{2.34}$$

We have (cf. [92]):

$$\lambda_n(c)<\frac{\sqrt{\pi}c^n(n!)^2}{(2n)!\Gamma(n+3/2)}:=\nu_n(c),\quad \forall c>0. \tag{2.35}$$

3 Numerics of PSWFs and prolate-differentiation schemes

In this section, we discuss the essential building blocks for spectral methods using PSWFs as basis functions. We start with introducing efficient algorithms for computing PSWFs and the associated eigenvalues $\{\chi_n(c)\}$ and $\{\lambda_n(c)\}$. We then introduce the prolate points, quadrature rules, prolate interpolation and pseudospectral differentiation in a manner analogue to the polynomial-based spectral algorithms [77]. More importantly, we highlight the Kong-Rokhlin's rule in [47] for paring up (c,N), and present a stable way to compute the approximate "inverse" of the pseudospectral differentiation in [96], which can lead to a well-conditioned prolate-collocation method for BVPs. We reiterate that PSWFs are non-polynomials, lacking some important properties of orthogonal polynomials, so some care must be taken to build and assemble these pieces of the puzzle.

3.1 Evaluation of PSWFs and the associated eigenvalues

Boyd [8] provided the algorithms and Matlab codes for computing the PSWFs, eigenvalues and their zeros etc.. The recent work [73] had deeper insights into the truncation of the infinite eigensystem where the Legendre-Galerkin method was applied to solve the Sturm-Liouville problem (2.21). One can refer to [66] for some delicate algorithms to enhance the codes in [8] for certain range of the parameters.

By expanding $\psi_n(x)$ in terms of orthonormal Legendre polynomials:

$$\psi_n(x)=\sum_{k=0}^{\infty}\beta_{nk}\overline{P}_k(x) \quad \text{with} \quad \beta_{nk}=\int_{-1}^{1}\psi_n(x)\overline{P}_k(x)dx, \tag{3.1}$$

we derive from the orthogonality the Parseval's identity:

$$\sum_{k=0}^{\infty}|\beta_{nk}|^2=1, \quad \forall\, n\geq 0. \tag{3.2}$$

By the parity, we have $\beta_{nk}=0$, if $n+k$ is odd. Inserting (3.1) into (2.21), we find from (2.19) and (2.23)-(2.25) that

$$\boldsymbol{A}\boldsymbol{\beta}_n=\chi_n\boldsymbol{\beta}_n, \quad \forall\, n\geq 0, \tag{3.3}$$

where $\boldsymbol{\beta}_n=(\beta_{n0},\beta_{n1},\cdots)^t$, and $\boldsymbol{A}=(a_{nk})$ is an infinite symmetric peta-diagonal matrix with non-zeros entries

$$\begin{aligned} a_{k,k}&=k(k+1)+\frac{2k(k+1)-1}{(2k+3)(2k-1)}\cdot c^2,\\ a_{k,k+2}&=a_{k+2,k}=\frac{(k+1)(k+2)}{(2k+3)\sqrt{(2k+1)(2k+5)}}\cdot c^2. \end{aligned} \tag{3.4}$$

The infinite system (3.3) can be decomposed into two symmetric tri-diagonal systems:

$$\boldsymbol{A}^e\boldsymbol{\beta}_n^e=\chi_n^e\boldsymbol{\beta}_n^e, \quad n=2l; \quad \boldsymbol{A}^o\boldsymbol{\beta}_n^o=\chi_n^o\boldsymbol{\beta}_n^o, \quad n=2l+1, \tag{3.5}$$

where $\boldsymbol{A}^e$ (resp. $\boldsymbol{A}^o$) consists of even-numbered (resp. odd-numbered) rows and columns of $\boldsymbol{A}$, and $\boldsymbol{\beta}_n^e=(\beta_{n0},\beta_{n2},\cdots)^t$ (resp. $\boldsymbol{\beta}_n^o=(\beta_{n1},\beta_{n3},\cdots)^t$).

In the computation, we have to reduce the infinite eigensystem (3.3). More precisely, to evaluate the first $(N+1)$-PSWFs and eigenvalues $\{\psi_n,\chi_n\}_{n=0}^N$, we approximate the PSWF by

$$\psi_n(x)\approx\sum_{k=0}^{M}\beta_{nk}\overline{P}_k(x), \tag{3.6}$$

with a suitable cut-off number $M>N$. Boyd [6] suggested a cut-off number for (3.6): $M\geq 2N+30$, which guaranteed a machine zero accuracy for computing $\{\chi_n(c),\psi_n(x;c)\}_{n=0}^N$ for all

$$0<c\leq c_*(N)=\frac{\pi}{2}\Big(N+\frac{1}{2}\Big). \tag{3.7}$$

Schmutzhard *et al.* [73] provided insightful observations on the choice of M for a prescribed accuracy.

We next present some stable formulas for computing the eigenvalues $\{\lambda_n(c)\}$ of the integral operator (see [92]), where we note that the magnitude of $\lambda_n(c)$ with $c>0$ is

exponentially small for large n. Taking $x=0$ in (2.13), and using (3.1) and the property $\overline{P}_0(x)=1/\sqrt{2}$, we have

$$\mathrm{i}^n\lambda_n(c)\psi_n(0;c)=\int_{-1}^{1}\psi_n(t;c)\,dt=\sqrt{2}\beta_{n0}. \tag{3.8}$$

The parity of PSWFs and the fact that $\psi_n(x;c)$ has exact n real roots in $(-1,1)$, imply that $\psi_n(0;c)\neq 0$ for even n, while $\psi_n(0;c)=0$ for odd n. Therefore, we can compute

$$\lambda_{2k}(c)=(-1)^k\frac{\sqrt{2}\beta_{2k,0}}{\psi_{2k}(0;c)},\quad k\geq 0. \tag{3.9}$$

To compute $\lambda_{2k+1}(c)$, we differentiate (2.13) with respect to x and then take $x=0$, leading to

$$\lambda_{2k+1}(c)=\frac{c}{\mathrm{i}^{2k}\partial_x\psi_{2k+1}(0;c)}\int_{-1}^{1}t\psi_{2k+1}(t;c)\,dt=(-1)^k\sqrt{\frac{2}{3}}\frac{c\beta_{2k+1,1}}{\partial_x\psi_{2k+1}(0;c)}. \tag{3.10}$$

In the above, we used (3.1) and $\overline{P}_1(t)=\sqrt{3/2}t$.

Remark 3.1. Although the magnitude of $\lambda_n(c)$ with $c>0$ is exponentially small for large n, its evaluation through (3.9)–(3.10) is stable since the values of $|\psi_{2k}(0;c)|$ and $|\partial_x\psi_{2k+1}(0;c)|$ are bounded away from zero for all k.

3.2 Kong-Rokhlin's rule

As already mentioned in the introductory section, it is important to choose the bandlimit parameter c to construct accurate approximation schemes on quasi-uniform grids. It is believed that one should choose c depending on N, and a quite safe choice is $c=N/2$ (see, e.g., [13, 92]).

Kong and Rokhlin [47] proposed a useful rule for pairing up c and N. The starting point is a prolate quadrature rule, say (3.21). We know from [101] that it has the accuracy for the complex exponential $e^{\mathrm{i}cax}$:

$$\Big|\int_{-1}^{1}e^{\mathrm{i}cax}\,dx-\sum_{j=0}^{N}e^{\mathrm{i}cax_j}\omega_j\Big|=O(\lambda_N). \tag{3.11}$$

Furthermore, for a bandlimited function of bandwidth c defined in (2.4) with $W=c$, we have (see [101, Remark 5.1])

$$\Big|\int_{-1}^{1}f(x)\,dx-\sum_{j=0}^{N}f(x_j)\omega_j\Big|\leq\varepsilon\|g\|_{L^2(-1,1)}, \tag{3.12}$$

where ε is the maximum error of integration of a single complex exponential as in (3.11). In view of this, Kong and Rokhlin [47] suggested the rule: given c and an error tolerance ε, choose the smallest integer $N_*=N_*(c,\varepsilon)$ such that

$$\lambda_{N_*}(c)\leq\varepsilon\leq\lambda_{N_*-1}(c). \tag{3.13}$$

Wang *et al.* [96] introduced a practical mean to implement this rule, which did not require computing the eigenvalues $\{\lambda_N\}$. The essential idea was to replace $\lambda_N(c)$ by its tight explicit bound, which converted the problem of finding N_* for given c and ε to locate the root of the algebraic equation: $F_\varepsilon(x;c)=0$ where

$$F_\varepsilon(x;c):=x\log\frac{ec}{4}-\Big(x+\frac{1}{2}\Big)\log\Big(x+\frac{1}{2}\Big)+\frac{1}{6x}+\log\frac{1}{\varepsilon}+\frac{1}{2}\log\frac{\pi e}{2},\quad x\geq 1. \tag{3.14}$$

As shown in [96], it has a unique root $x_*>1$, so we take $N_*=[x_*]$ (i.e., the integer part of x_*).

3.3 Prolate points and prolate quadrature

The grid points of spectral and spectral-element methods are usually chosen as nodes of a certain Gaussian quadrature rule, which enjoys the highest degree of precision (DOP) for polynomials. For example, let $\{\xi_j\}_{j=0}^N$ be the Legendre-Gauss-Lobatto (LGL) points (i.e., zeros of $(1-x^2)P_N'(x)$), and $\{\rho_j\}_{j=0}^N$ be the corresponding quadrature weights given by

$$\rho_j=\frac{2}{N(N+1)}\frac{1}{P_N^2(x_j)},\quad 0\leq j\leq N. \tag{3.15}$$

Then the LGL quadrature has the exactness (see, e.g., [11,77]):

$$\int_{-1}^{1}P_n(x)dx=\sum_{j=0}^{N}P_n(\xi_j)\rho_j,\quad 0\leq n\leq 2N-1, \tag{3.16}$$

which, in other words, is exact for all $v\in\mathcal{P}_{2N-1}$ (the set of all algebraic polynomials of degree at most $2N-1$). It is known from the standard textbook on numerical analysis that Euclidean division of polynomials plays an essential role in the context of Gaussian quadrature. Basically, for every pair of polynomials (s,p) such that $p\neq 0$, polynomial division provides a quotient q and a remainder r such that

$$s(x)=p(x)q(x)+r(x), \tag{3.17}$$

and either $r=0$ or $\deg(r)<\deg(q)$. Moreover, (q,r) is the unique pair of polynomials having this property.

Unfortunately, the property (3.17) does not hold for PSWFs. Moreover, unlike polynomials, the operations in (3.19) below are not closed in the vector space

$$V_N^c=\text{span}\big\{\psi_n(x;c):0\leq n\leq N\big\}. \tag{3.18}$$

That is, for any $\psi_n,\psi_m\in V_N^c$,

$$\partial_x\psi_n\notin V_{N-1}^c,\quad \int\psi_n dx\notin V_{N+1}^c,\quad \psi_n\cdot\psi_m\notin V_{2N}^c,\quad \forall\, c>0. \tag{3.19}$$

In view of (3.19), we can not expect to have a "perfect" quadrature rule like (3.16). In practice, several rules have been proposed (see, e.g., [7,101] and [66, Ch. 9]).

- The first is to pursue the highest DOP over the $2N$-dimensional space V^c_{2N-1} (cf. [6, 7]). More precisely, we fix $x_0=-1, x_N=1$, and search for quadrature nodes $\{x_j\}_{j=1}^{N-1}$ and weights $\{\omega_j\}_{j=0}^N$ such that

$$\int_{-1}^1 \psi_n(x)dx=\psi_n(-1)\omega_0+\sum_{j=1}^{N-1}\psi_n(x_j)\omega_j+\psi_n(1)\omega_N,\quad 0\le n\le 2N-1. \tag{3.20}$$

  This requires to solve a nonlinear system to compute the nodes and weights. We refer to Boyd [6] for the detailed algorithm and codes.

- A second proposal is to choose the nodes $\{x_j\}_{j=0}^N$ as zeros of $(1-x^2)\partial_x\psi_N(x)$ (see, e.g., [8, 13, 51]), analogue to the LGL case, which are therefore referred to as the prolate-Lobatto (PL) points. The quadrature weights $\{\omega_j\}_{j=0}^N$ are determined by

$$\int_{-1}^1 \psi_n(x)dx=\sum_{j=0}^N\psi_n(x_j)\omega_j,\quad 0\le n\le N, \tag{3.21}$$

  where by (3.8), the integral on the left side is $\sqrt{2}\beta_{n0}$. Note that this rule only has a DOP over V^c_N, but not over V^c_{2N-1} as for polynomials.

  We remark that Xiao *et al.* [101, Thm. 6.3] considered the Guassian rule (where the nodes were zeros of ψ_{N+1}) and analysed the quadrature error for general continuous functions based on the Euclidean division of bandlimited functions.

- Osipov and Rokhlin [65] proposed a prolate-Gaussian quadrature by taking the nodes $\{x_j\}_{j=0}^N$ as zeros of $\psi_{N+1}(x)$ and computing the weights via

$$\omega_j=\int_{-1}^1\frac{\psi_{N+1}(x)}{\psi'_{N+1}(x)(x-x_j)}dx,\quad 0\le j\le N. \tag{3.22}$$

  Although it lacks the exactness like (3.21), it can be shown

$$\left|\int_{-1}^1\psi_n(x)dx-\sum_{j=0}^N\psi_n(x_j)\omega_j\right|\le\lambda_{N+1}\big(6\chi_{N+1}-24\log\lambda_{N+1}\big),\quad 0\le n\le N. \tag{3.23}$$

  Note that one can extend this rule to the Lobatto quadrature.

We see from the above that it is necessary to compute the zeros of PSWF or the derivative of PSWF. Boyd [8] described the Newton's iteration method with some care in selecting initial guesses. Alternatively, one can use the general algorithm in [25] for computing zeros of special functions satisfying the differential equation:

$$p(x)u''(x)+q(x)u'(x)+r(x)u(x)=0,$$

where p,q,r are quadratic polynomials. Indeed, the Sturm-Liouville problem (2.21) falls into this category. With the zeros of ψ_n, one can locate the zeros of ψ_N' by Newton's iteration with the initial guess $\{(t_j+t_{j+1})/2\}_{j=1}^{N-1}$, where $\{t_j\}_{j=1}^N$ are zeros of ψ_N. In fact, as shown in [66], ψ_n' has $n-1$ zeros in $(-1,1)$ that interlace with n zeros of ψ_n, when $\chi_n > c^2$.

Remark 3.2. In the context of prolate pseudospectral/collocation approaches, there is very subtle difference between the sets of points (also see [13]). Hereafter, we shall restrict to the PL points.

3.4 Prolate interpolation, cardinal basis and pseudospectral differentiation

Let $\{x_j\}_{j=0}^N$ be the PL points and V_N^c be the space defined in (3.18). Consider the prolate-interpolation problem:

$$\text{Find } p\in V_N^c \quad \text{such that} \quad p(x_j)=u(x_j), \quad 0\le j\le N, \tag{3.24}$$

for any $u\in C[-1,1]$. Like polynomial interpolation, we define the interpolation operator: $\mathcal{I}_N^c: C[-1,1]\to V_N^c$ by

$$(\mathcal{I}_N^c u)(x)=\sum_{k=0}^N u(x_k)h_k(x;c), \tag{3.25}$$

where the cardinal basis functions $h_k\in V_N^c$ and satisfy

$$h_k(x_j;c)=\delta_{kj}, \quad 0\le k,j\le N, \ \ c>0. \tag{3.26}$$

If c=0, they reduce to the Lagrange basis polynomials associated with LGL points $\{\xi_k\}_{k=0}^N$:

$$\tilde{h}_k(x)=\frac{s(x)}{s'(\xi_k)(x-\xi_k)}, \ \ 0\le k\le N \quad \text{with} \quad s(x)=(1-x^2)P_N'(x). \tag{3.27}$$

Alternatively, we have the representation:

$$\tilde{h}_k(x)=\sum_{j=0}^N \frac{\rho_k}{\tilde{\gamma}_j}P_j(\xi_k)P_j(x), \quad 0\le j\le N, \tag{3.28}$$

where $\{\rho_k\}$ are LGL quadrature weights defined in (3.15), $\tilde{\gamma}_j=2/(2j+1)$ for $0\le j\le N-1$, and $\tilde{\gamma}_N=2/N$.

When it comes to PSWFs, the representations (3.27) and (3.28) are not equivalent. Following (3.28), we write

$$h_k(x)=\sum_{n=0}^N t_{nk}\psi_n(x), \tag{3.29}$$

and determine $\{t_{nk}\}$ from the interpolation conditions (3.26). More precisely, introducing the matrices $\boldsymbol{\Psi}^{(m)},\boldsymbol{T},\boldsymbol{D}^{(m)}\in\mathbb{R}^{(N+1)\times(N+1)}$ with the entries

$$\boldsymbol{\Psi}^{(m)}_{jk}=\psi^{(m)}_k(x_j),\quad \boldsymbol{T}_{nk}=t_{nk},\quad \boldsymbol{D}^{(m)}_{jk}=h^{(m)}_k(x_j), \tag{3.30}$$

and denoting $\boldsymbol{\Psi}=\boldsymbol{\Psi}^{(0)}$, we have $\boldsymbol{\Psi}\boldsymbol{T}=\boldsymbol{I}_{N+1}$, so $\boldsymbol{T}=\boldsymbol{\Psi}^{-1}$. By (3.29), the mth-order prolate differentiation matrix is computed by

$$\boldsymbol{D}^{(m)}=\boldsymbol{\Psi}^{(m)}\boldsymbol{\Psi}^{-1},\quad m\geq 1, \tag{3.31}$$

where for $m=0$, we have $\boldsymbol{D}^{(0)}=\boldsymbol{I}_{N+1}$. It implies

$$\boldsymbol{D}^{(m)}\boldsymbol{\Psi}=\boldsymbol{\Psi}^{(m)},\quad \boldsymbol{D}^{(m)}\boldsymbol{\phi}=\boldsymbol{\phi}^{(m)}, \tag{3.32}$$

where for any $\phi\in V^c_N$, $\boldsymbol{\phi}^{(m)}=(\phi^{(m)}(x_0),\cdots,\phi^{(m)}(x_N))^t$ and $\boldsymbol{\phi}=\boldsymbol{\phi}^{(0)}$.

Following (3.27), we define

$$l_k(x)=\frac{s(x)}{s'(x_k)(x-x_k)},\quad 0\leq k\leq N\quad\text{with}\quad s(x)=(1-x^2)\psi'_N(x). \tag{3.33}$$

One verifies readily that for $c>0$,

$$l_k(x_j)=\delta_{jk},\quad 0\leq k,j\leq N,\quad\text{but}\quad l_k\notin V^c_N,\quad 0\leq k\leq N. \tag{3.34}$$

Correspondingly, we define the mth-order differentiation matrix $\widehat{\boldsymbol{D}}^{(m)}$ with the entries $\widehat{\boldsymbol{D}}^{(m)}_{jk}=l^{(m)}_k(x_j)$ for $0\leq k,j\leq N$. We refer to [96, Appendix A] for the explicit formulas for the entries of $\widehat{\boldsymbol{D}}^{(1)}$ and $\widehat{\boldsymbol{D}}^{(2)}$, which only involve the function values $\{\psi_N(x_j)\}_{j=0}^N$.

In what follows, let $\boldsymbol{D}^{(2)}_{\text{in}}\in\mathbb{R}^{(N-1)\times(N-1)}$ be the matrix obtained by deleting the first and last rows and columns of $\boldsymbol{D}^{(2)}$, and likewise for $\widehat{\boldsymbol{D}}^{(2)}_{\text{in}}$.

3.5 "Inverse" of prolate pseudospectral differentiation matrix

In this section, we review the approach in [96] for computing the approximate "inverse" of $\boldsymbol{D}^{(2)}_{\text{in}}$ or $\widehat{\boldsymbol{D}}^{(2)}_{\text{in}}$ in a stable manner. With this, we can precondition the prolate-collocation method, leading to well-conditioned collocation schemes. Moreover, we can derive a new basis in the course from which we can also construct well-conditioned collocation methods.

We essentially extend the idea for polynomials in [19,34,93] to the PSWFs. That is, we look for a matrix $\boldsymbol{B}_{\text{in}}\in\mathbb{R}^{(N-1)\times(N-1)}$ such that

$$\boldsymbol{D}^{(2)}_{\text{in}}\boldsymbol{B}_{\text{in}}\approx\boldsymbol{I}_{N-1},\quad \boldsymbol{B}_{\text{in}}\boldsymbol{D}^{(2)}_{\text{in}}\approx\boldsymbol{I}_{N-1}, \tag{3.35}$$

DOI https://doi.org/10.4208/jms.v50n2.17.01 | Generated on 2024-11-19 16:37:05

for large N, and likewise for $\widehat{\boldsymbol{D}}_{\rm in}^{(2)}$. Such a matrix is generated from a new basis obtained from the generalised Birkhoff interpolation. Let $\{x_j\}_{j=0}^N$ be the PL points with $x_0=-x_N=-1$. Define

$$B_0(x)=\frac{1-x}{2},\quad B_N(x)=\frac{1+x}{2}, \tag{3.36}$$

and for $1\le k\le N-1$, we look for

$$B_k\in W_N^{c,0}:=\text{span}\big\{\phi_n:\phi_n''(x)=\psi_n(x)\text{ with }\phi_n(\pm1)=0,\,0\le n\le N-2\big\}, \tag{3.37}$$

such that

$$B_k''(x_j)=\delta_{jk},\quad 1\le j\le N-1,\quad B_k(\pm1)=0,\quad 1\le k\le N-1. \tag{3.38}$$

By construction, the new basis $\{B_k\}$ is associated with the generalized Birkhoff interpolation problem, that is, given $u\in C^2(-1,1)$, find $p\in W_N^{c,0}\cup\mathcal{P}_1$ such that

$$p(-1)=u(-1);\quad p''(x_j)=u''(x_j),\,1\le j\le N-1;\quad p(1)=u(1), \tag{3.39}$$

as we can express the interpolant as

$$p(x)=u(-1)B_0(x)+\sum_{k=1}^{N-1}u''(x_k)B_k(x)+u(1)B_N(x). \tag{3.40}$$

We first consider how to compute the new basis $\{B_k\}$. Solving the ordinary differential equation in (3.37) directly leads to

$$\phi_n(x)=x\int_{-1}^x\psi_n(t)dt-\int_{-1}^x t\psi_n(t)dt+\frac{1+x}{2}\int_{-1}^1(t-1)\psi_n(t)dt. \tag{3.41}$$

Then we compute $\{B_k\}_{k=1}^{N-1}$, by writing

$$B_k(x)=\sum_{n=0}^{N-2}\alpha_{nk}\phi_n(x),\quad\text{so}\quad B_k''(x)=\sum_{n=0}^{N-2}\alpha_{nk}\psi_n(x). \tag{3.42}$$

Thus we can find the coefficients $\{\alpha_{nk}\}$ by $B_k''(x_j)=\delta_{jk}$ with $1\le k,j\le N-1$, that is,

$$\boldsymbol{A}=\bar{\boldsymbol{\Psi}}^{-1}\quad\text{where}\quad\boldsymbol{A}_{nk}=\alpha_{nk},\quad\bar{\boldsymbol{\Psi}}_{jn}=\psi_n(x_j), \tag{3.43}$$

for $1\le j,k\le N-1$ and $0\le n\le N-2$. Thus, we can compute $\{B_k\}$ by (3.42). Define the matrices

$$\boldsymbol{B}=(b_{ij})_{0\le i,j\le N},\quad\boldsymbol{B}_{\rm in}=(b_{ij})_{1\le i,j\le N-1},\quad b_{ij}:=B_j(x_i). \tag{3.44}$$

Now, we justify (3.35). Let $\mathcal{I}_N^c$ be the prolate-interpolation operator defined in (3.25). Clearly, we have

$$\mathcal{I}_N^cB_k(x)=\sum_{j=0}^N B_k(x_j)h_j(x;c), \tag{3.45}$$

DOI https://doi.org/10.4208/jms.v50n2.17.01 | Generated on 2024-11-19 16:37:05

and for $1\le k\le N-1$,

$$(\mathcal{I}_N^c B_k)''(x_i)=\sum_{j=0}^{N} B_k(x_j)h_j''(x_i;c)=\sum_{j=1}^{N-1} B_k(x_j)h_j''(x_i;c),\quad 1\le i\le N-1, \tag{3.46}$$

where in the last step, we used the fact: $B_k(\pm 1)=0$.

Let

$$e_k(x)=\mathcal{I}_N^c B_k(x)-B_k(x).$$

With this, we derive from (3.38) and (3.46) that

$$e_k''(x_i)+\delta_{ik}=\sum_{j=1}^{N-1} B_k(x_j)h_j''(x_i;c),\quad 1\le i,k\le N-1, \tag{3.47}$$

This implies

$$\boldsymbol{D}_{\rm in}^{(2)}\boldsymbol{B}_{\rm in}-\boldsymbol{I}_{N-1}=\boldsymbol{E}^{(2)},\quad \boldsymbol{E}^{(2)}=(e_k''(x_i))_{1\le i,k\le N-1}. \tag{3.48}$$

Note that the entries of $\boldsymbol{E}^{(2)}$ are the second derivative of prolate-interpolation errors of $\{B_k\}$ (which are analytic functions). It is expected that they decay exponentially when N is large. However, the estimate of interpolation error $\mathcal{I}_N^c u-u$ remains open, though we can estimate the L^2-orthogonal projection error (see, e.g., [13, 95]). We therefore have the first relation in (3.35).

In fact, we can justify the second relation of (3.35) in a similar fashion. Let $\widetilde{\mathcal{I}}_N^c$ be the generalized Birkhoff-interpolation operator associated with (3.39), i.e., $\widetilde{\mathcal{I}}_N^c u=p$ in (3.40). Therefore, for $1\le j\le N-1$, we can write

$$\widetilde{\mathcal{I}}_N^c h_j(x_i)=\sum_{k=1}^{N-1} h_j''(x_k)B_k(x_i),\quad 1\le i\le N-1, \tag{3.49}$$

so similarly, we understand the "approximately equal" in (3.35) due to the interpolation errors: $(\widetilde{\mathcal{I}}_N^c h_j-h_j)(x_i)$.

Remark 3.3. The above approach also applies to the cardinal basis $\{l_j\}$ and the corresponding prolate-differentiation matrix $\widehat{\boldsymbol{D}}_{\rm in}^{(2)}$.

We demonstrate in Figure 1 (see [96, Fig. 3.4]) the growth of the magnitude of the largest and smallest eigenvalues of $\boldsymbol{D}_{\rm in}^{(2)}$ and $\widehat{\boldsymbol{D}}_{\rm in}^{(2)}$, compared with the Legendre case, where (c,N) is once again paired up by the approximate Kong-Rokhlin's rule. We observe a much slower growth of the largest eigenvalue, so the condition number of the differentiation matrix is much smaller. We also see that the magnitude of the smallest eigenvalue behaves like a constant.

We depict in Figure 2 (see [96, Fig. 5.1]) the distribution of the largest and smallest eigenvalues of $\boldsymbol{B}_{\rm in}\boldsymbol{D}_{\rm in}^{(2)}$ and $\boldsymbol{B}_{\rm in}\widehat{\boldsymbol{D}}_{\rm in}^{(2)}$ at the PL points. We see that all their eigenvalues for

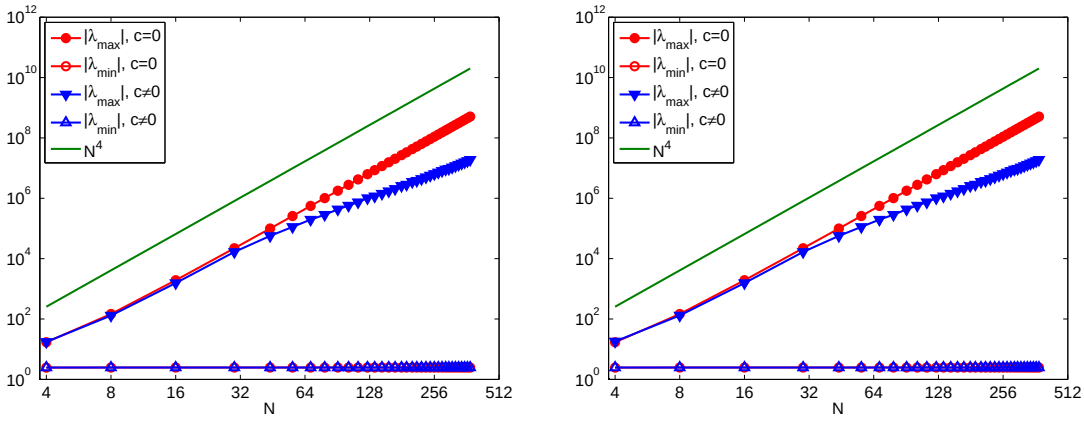

Figure 1: Growth of the magnitude of the largest and smallest eigenvalues of $\boldsymbol{D}_{\text{in}}^{(2)}$ (left) and $\widehat{\boldsymbol{D}}_{\text{in}}^{(2)}$ (right) at the PL points ($c\neq 0$) against the Legendre case at the LGL points ($c=0$).

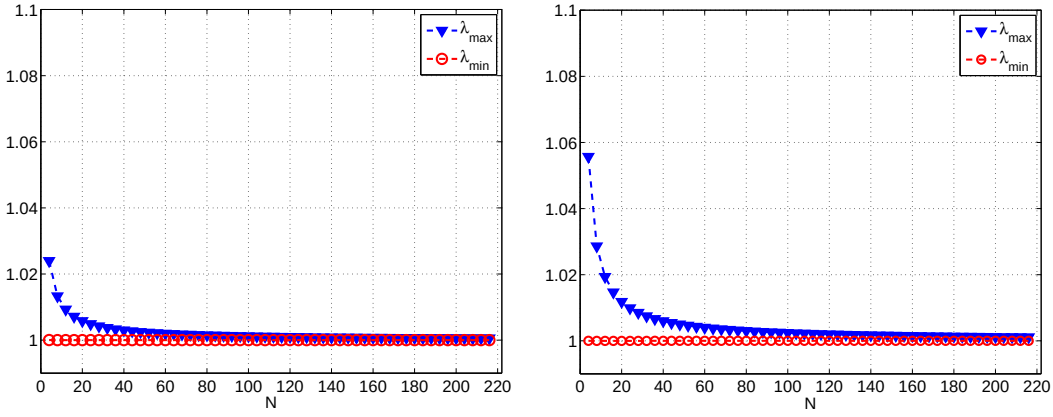

Figure 2: Distribution of the largest and smallest eigenvalues of $\boldsymbol{B}_{\text{in}}\boldsymbol{D}_{\text{in}}^{(2)}$ (left) and $\boldsymbol{B}_{\text{in}}\widehat{\boldsymbol{D}}_{\text{in}}^{(2)}$ (right) for various $N\in[4,218]$ and $c=N/2$.

various N with $c=N/2$ are confined in $[\lambda_{\min},\lambda_{\max}]$, which are concentrated around one for slightly large N. This agrees with (3.35).

With the new basis $\{B_j\}$ at our disposal, we can directly use it as a basis for prolate-collocation solutions of PDEs and can also precondition the usual prolate-collocation schemes (see [96]), which we will outline in Section 5.

DOI https://doi.org/10.4208/jms.v50n2.17.01 | Generated on 2024-11-19 16:37:05

3.6 Kong-Rokhlin's prolate-spectral differentiation schemes

In Kong and Rokhlin [47], highly accurate numerical differentiation schemes via PSWFs were introduced to approximate bandlimited functions, and the involved differentiation matrices have spectral radii that grow asymptotically $O(M)$ and $O(M^2)$, for first and second derivatives, respectively, where M is the dimension of the matrix. To this end, we have a brief review of the method therein.

Let $\{\zeta_j,\varpi_j\}_{j=1}^M$ be a set of quadrature nodes and weights of a rule that integrates exactly all pairwise products of $\psi_0,\cdots,\psi_{N-1}\in V_{N-1}^c$, that is,

$$\int_{-1}^{1}\psi_k(x)\psi_l(x)dx=\sum_{j=1}^{M}\psi_k(\zeta_j)\psi_l(\zeta_j)\varpi_j,\quad \forall\psi_k,\psi_l\in V_{N-1}^c, \tag{3.50}$$

which can be found in [101]. Equivalently, by the orthogonality of PSWFs, we have from (3.50) that

$$\widetilde{\boldsymbol{\Psi}}^t\widetilde{\boldsymbol{\Psi}}=\boldsymbol{I}_N,\quad \text{where}\quad \widetilde{\boldsymbol{\Psi}}=\big(a_{jk}:=\sqrt{\varpi_j}\psi_{k-1}(x_j)\big)_{1\le j\le M}^{1\le k\le N}. \tag{3.51}$$

For any $u_N\in V_{N-1}^c$, we write

$$u_N(x)=\sum_{n=0}^{N-1}\beta_n\psi_n(x)\ \text{ and }\ u_N(\zeta_j)=\sum_{n=0}^{N-1}\beta_n\psi_n(\zeta_j),\quad 1\le j\le M. \tag{3.52}$$

Therefore, we have the matrix form

$$\boldsymbol{W}\boldsymbol{u}=\widetilde{\boldsymbol{\Psi}}\boldsymbol{\beta}, \tag{3.53}$$

where

$$\boldsymbol{W}=\mathrm{diag}(\varpi_1,\cdots,\varpi_M),\quad \boldsymbol{u}=(u_N(\zeta_1),\cdots,u_N(\zeta_M))^t,\quad \boldsymbol{\beta}=(\beta_0,\cdots,\beta_{N-1})^t. \tag{3.54}$$

Thus, using (3.51), we compute the expansion coefficients from (3.53) by

$$\boldsymbol{\beta}=\widetilde{\boldsymbol{\Psi}}^t\boldsymbol{W}\boldsymbol{u}. \tag{3.55}$$

As pointed out [47], we choose $M>N$ to guarantee the accuracy of the quadrature rule (3.50). However, in the Legendre case, we can take $M=N$.

Then the prolate-spectral differentiation scheme is given by

$$u_N^{(k)}(\zeta_j)=\sum_{n=0}^{N-1}\beta_n\psi_n^{(k)}(\zeta_j),\quad 1\le j\le M,\ k\ge 1, \tag{3.56}$$

with the matrix notation:

$$\boldsymbol{u}^{(k)}=\boldsymbol{\Psi}^{(k)}\widetilde{\boldsymbol{\Psi}}^t\boldsymbol{W}\boldsymbol{u},\quad k\ge 1,\ \text{where}\ \boldsymbol{\Psi}^{(k)}=\big(\psi_{i-1}^{(k)}(x_j)\big)_{1\le j\le M}^{1\le i\le N}, \tag{3.57}$$

and $\boldsymbol{u}^{(k)}$ is a column-M vector of the kth-order derivative values as defined in (3.54). Note that $\boldsymbol{\Psi}^{(0)}=\boldsymbol{W}^{-1}\widetilde{\boldsymbol{\Psi}}$. The kth-order differentiation matrix is defined by

$$\widetilde{\boldsymbol{D}}^{(k)}:=\boldsymbol{\Psi}^{(k)}\widetilde{\boldsymbol{\Psi}}^{t}\boldsymbol{W},\quad k\geq 1. \tag{3.58}$$

In practice, we need to construct differentiation matrices that incorporate boundary conditions, e.g., $u(\pm 1)=0$ for second-order boundary value problems. Kong and Rokhlin [47] suggested a new modal basis

$$\phi_j(x)=\psi_j(x)-\mu_j(x),\quad \text{where}\quad \mu_j(x)=\psi_j(-1)\frac{1-x}{2}+\psi_j(1)\frac{1+x}{2}, \tag{3.59}$$

which apparently satisfies $\phi_j(\pm 1)=0$, for all $j\geq 0$. To have the property (3.51), we first apply the algorithm in [101] to construct a quadrature rule similar to (3.50), and the pivoted Gram-Schmidt re-orthogonalization process. It was also shown that the new differentiation scheme together with the Kong-Rokhlin's rule for pairing up (c,N) outperformed the polynomial methods in the sense: (i) significantly better approximation to the continuous spectrum of the eigenproblem; and (ii) better conditioning of the differentiation matrix, e.g., with a growth $O(M^2)$ for $k=2$.

3.7 Novel differentiation schemes based on generalised PSWFs

In what follows, we introduce a new spectral-differentiation scheme using a modal basis obtained from the generalised PSWFs [94]. The significant features reside in that

- The new basis naturally incorporates the boundary conditions, and can be directly computed from the generalised PSWFs in [94];
- The conditioning of the prolate differentiation matrix, e.g., the second-order, grows like c^2;
- It enjoys spectral accuracy on quasi-uniform grids.

Below, we just consider the method for second-order equations, and refer to the readers to [106] for the details.

We are essentially motivated by the well-conditioned Legendre-spectral-Galerkin methods using integrated Legendre polynomials as basis functions [76] for second-order BVPs, which are later systematically extended to generalized Jacobi polynomials/functions for general BVPs in [31,32]. Recall the following important property (see, e.g., [77]):

$$\begin{aligned}\varphi_k(x):&=\int_{-1}^{x}P_{k-1}(y)dy=\frac{1}{2k-1}\big(P_k(x)-P_{k-2}(x)\big)\\&=\frac{1}{2(k-1)}(x^2-1)P_{k-2}^{(1,1)}(x)=\frac{2}{k-1}P_k^{(-1,-1)}(x),\quad k\geq 2,\end{aligned} \tag{3.60}$$

where we refer to [87] for the Jacobi polynomials $P_k^{(\alpha,\beta)}(x)$ with parameters α or $\beta\leq -1$. We highlight some attractive properties of the new basis $\{\varphi_k\}_{k\geq 2}$:

(i) We have $\psi_k(\pm1)=0$ for all $k\geq1$, and the orthogonality:

$$\int_{-1}^{1}\varphi_k'(x)\varphi_j'(x)dx=\int_{-1}^{1}\varphi_k(x)\varphi_j(x)(1-x^2)^{-1}dx=0,\quad k\neq j,\ k,j\geq2. \tag{3.61}$$

Notably, under this basis, the matrix resulted from the leading term u'' of the Galerkin formulation is diagonal, so the resulted system is well-conditioned. Actually, it forms an optimal basis in $H_0^1(-1,1)$.

(ii) If we define

$$\varphi_0(x)=1,\quad \varphi_1(x)=\int_{-1}^{x}P_0(y)dy=1+x, \tag{3.62}$$

then $\{\varphi_k\}_{k\geq0}$ forms an H^1-basis.

(iii) Using the notion of generalized Jacobi polynomials leads to much concise and precise analysis and estimates of the spectral approximations (see [77, Ch. 6]).

Wang and Zhang [94] generalized the PSWFs of order zero to an orthogonal system with respect to the Gegenbauer weight function $\omega_\alpha(x)=(1-x^2)^\alpha$ with $\alpha>-1$. The generalized PSWFs are eigenfunctions of the singular Sturm-Liouville problem:

$$-(1-x^2)^{-\alpha}\partial_x\big((1-x^2)^{\alpha+1}\partial_x\psi_n^{(\alpha)}(x;c)\big)+c^2x^2\psi_n^{(\alpha)}(x;c)=\chi_n^{(\alpha)}(c)\psi_n^{(\alpha)}(x;c), \tag{3.63}$$

for $c>0,\alpha>-1$ and $n\geq0$. They are mutually orthogonal

$$\int_{-1}^{1}\psi_m^{(\alpha)}(x;c)\psi_n^{(\alpha)}(x;c)\omega_\alpha(x)dx=\delta_{mn}, \tag{3.64}$$

and form a complete system in $L^2_{\omega_\alpha}(-1,1)$. When $c=0$, they reduce to Gegenbauer polynomials. Notably, they are also eigenfunctions of the integral operator:

$$\mathrm{i}^n\lambda_n^{(\alpha)}\psi_n^{(\alpha)}(x;c)=\int_{-1}^{1}\psi_n^{(\alpha)}(t;c)e^{\mathrm{i}ctx}\omega_\alpha(t)dt,\quad\forall x\in(-1,1). \tag{3.65}$$

We refer to [94] for many other properties.

Inspired by (3.60), we introduce

$$q_n(x)=(1-x^2)\psi_{n-2}^{(1)}(x;c),\quad n\geq2, \tag{3.66}$$

which obviously meets $q_n(\pm1)=0$. It follows from (3.64) the orthogonality:

$$\int_{-1}^{1}q_n(x)q_m(x)(1-x^2)^{-1}dx=\delta_{mn}. \tag{3.67}$$

We derive from (3.63) with $\alpha=1$ the following important property:

$$-q_n''(x)-c^2q_n(x)=\sigma_n(1-x^2)^{-1}q_n(x)=\sigma_n\psi_{n-2}^{(1)}(x;c),\quad n\geq2, \tag{3.68}$$

where

$$\sigma_n := \sigma_n(c) = \chi^{(1)}_{n-2}(c) - c^2 + 2. \tag{3.69}$$

Like (3.62), we define

$$q_0(x) = \cos cx, \quad q_1(x) = \sin cx, \tag{3.70}$$

which turn to be the eigenfunctions of (3.68) corresponding to the eigenvalues $\sigma_0 = \sigma_1 = 0$. With this, one can expand general functions.

Denote

$$Y^c_N := \text{span}\{q_n : 0 \le n \le N\}, \quad Y^{c,0}_N := \text{span}\{q_n : 2 \le n \le N\}. \tag{3.71}$$

We now formulate the differentiation scheme for functions in Y^c_N. For any $v_N \in Y^c_N$, we write

$$v_N(x) = \hat{v}_0 q_0(x) + \hat{v}_1 q_1(x) + \sum_{n=2}^{N} \hat{v}_n q_n(x). \tag{3.72}$$

Let $\{x_j\}_{j=0}^N$ (with $x_0 = -x_N = -1$) be the PL points as before. Like computing the cardinal basis in (3.29), we can find $\{\hat{v}_n\}$ by

$$\hat{\boldsymbol{v}} = \boldsymbol{Q}^{-1}\boldsymbol{v}, \quad \boldsymbol{Q} = (q_n(x_j))_{0\le j,n\le N}, \tag{3.73}$$

where $\hat{\boldsymbol{v}}$ and $\boldsymbol{v}$ are column-$N+1$ vectors of $\{\hat{v}_n\}$ and $\{v_N(x_j)\}$, respectively.

It is clear that $\hat{v}_0$ and $\hat{v}_N$ can be computed directly by taking $x = \pm 1$, so we have

$$v^*_N(x) := \hat{v}_0 q_0(x) + \hat{v}_1 q_1(x) = \frac{v_N(1) - v_N(-1)}{2} \frac{\cos cx}{\cos c} + \frac{v_N(1) + v_N(-1)}{2} \frac{\sin cx}{\sin c}, \tag{3.74}$$

and

$$(v_N - v^*_N)(x) = \sum_{n=2}^{N} \hat{v}_n q_n(x) \in Y^{c,0}_N. \tag{3.75}$$

Thus, by (3.66) and (3.67),

$$\hat{v}_n = \int_{-1}^{1} (v_N - v^*_N)(x) q_n(x) (1-x^2)^{-1} dx = \int_{-1}^{1} (v_N - v^*_N)(x) \psi^{(1)}_{n-2}(x)\, dx, \tag{3.76}$$

which requires an accurate numerical quadrature.

We extend (3.68) to $n = 0,1$ with the understanding of $\sigma_0 = \sigma_1 = 0$ and $\psi^{(1)}_{-2} = \psi^{(1)}_{-1} = 0$. Then we have the matrix equation:

$$-\boldsymbol{Q}^{(2)} - c^2 \boldsymbol{Q} = \widehat{\boldsymbol{\Psi}} \boldsymbol{\Sigma}, \tag{3.77}$$

where

$$\boldsymbol{Q}^{(k)} = (q^{(k)}_n(x_j))_{0\le j,n\le N}, \quad \widehat{\boldsymbol{\Psi}} = \left(\psi^{(1)}_{n-2}(x_j)\right)_{0\le j,n\le N}, \quad \boldsymbol{\Sigma} = \text{diag}(\sigma_0, \cdots, \sigma_N). \tag{3.78}$$

Then the differentiation scheme based on (3.72) reads

$$\boldsymbol{v}^{(k)}=\boldsymbol{Q}^{(k)}\hat{\boldsymbol{v}}=\boldsymbol{Q}^{(k)}\boldsymbol{Q}^{-1}\boldsymbol{v}=:\widetilde{\boldsymbol{D}}^{(k)}\boldsymbol{v},\quad k\geq 1. \tag{3.79}$$

In particular, for $k=2$, we can simplify it to

$$\widetilde{\boldsymbol{D}}^{(2)}=-c^2\boldsymbol{I}_{N+1}-\widehat{\boldsymbol{\Psi}}\boldsymbol{\Sigma}\boldsymbol{Q}^{-1}. \tag{3.80}$$

Note that it does not involves the derivative values of generalised PSWFs.

We next look at this from the perspective of prolate-Galerkin formulation. This involves the stiffness and mass matrices under the new basis of $Y_N^{c,0}$, that is, $\boldsymbol{S}=(s_{jn})_{2\leq j,n\leq N}$ and $\boldsymbol{M}=(m_{jn})_{2\leq j,n\leq N}$, with

$$s_{jn}:=\int_{-1}^{1}q_n'(x)q_j'(x)dx,\quad m_{jn}:=\int_{-1}^{1}q_n(x)q_j(x)dx. \tag{3.81}$$

It follows from (3.68) that

$$\boldsymbol{S}=c^2\boldsymbol{M}+\widetilde{\boldsymbol{\Sigma}},\quad \text{where}\quad \widetilde{\boldsymbol{\Sigma}}=\text{diag}(\sigma_2,\cdots,\sigma_N). \tag{3.82}$$

This attractive property is essential for efficient prolate-spectral algorithms for second-order BVPs (cf. Section 5).

4 Spectral approximation results

In this section, we review the results on error estimates of spectral approximation of bandlimited functions and general functions in Sobolev spaces by PSWF expansions.

Let us start with introducing some notation. Let $\Lambda=(-1,1)$, and $\omega(x)>0$ be a generic weight function on Λ. Denote by $L^2_\omega(\Lambda)$ the square integrable functions with the norm $\|\cdot\|_\omega$. Further, let $H^s_\omega(\Lambda)$ with integer s be the usual Sobolev space with the norm $\|\cdot\|_{s,\omega}$ and semi-norm $|\cdot|_{s,\omega}$. Whenever $\omega\equiv 1$, we drop the weight function from the above notation.

For any $u\in L^2(\Lambda)$, we write

$$u(x)=\sum_{n=0}^{\infty}\hat{u}_n\psi_n(x;c)\quad\text{where}\quad \hat{u}_n:=\hat{u}_n(c)=\int_{-1}^{1}u(x)\psi_n(x;c)dx. \tag{4.1}$$

We consider the approximation of u by its L^2-projection $\pi_N^c u\in V_N^c$ (defined in (3.18)):

$$\int_{-1}^{1}(u-\pi_N^c u)(x)v(x)dx=0,\quad \forall v\in V_N^c. \tag{4.2}$$

It is clear that we have

$$(\pi_N^c u)(x)=\sum_{n=0}^{N}\hat{u}_n\psi_n(x;c). \tag{4.3}$$

DOI https://doi.org/10.4208/jms.v50n2.17.01 | Generated on 2024-11-19 16:37:05

As a Riesz basis in $L^2(\Lambda)$, we have that for any $c>0$,

$$\|\pi_N^c u-u\|\to 0 \quad \text{as} \quad N\to\infty. \tag{4.4}$$

An important issue is to understand *for what range of c, the PSWF expansion enjoys spectral accuracy on quasi-uniform grids.*

4.1 *c*-bandlimited functions

We first consider the PSWF approximation of c-bandlimited functions, defined by

$$u(x)=\int_{-1}^{1} e^{\mathrm{i}cxt}\phi(t)dt, \quad \text{for } \phi\in L^2(\Lambda). \tag{4.5}$$

It is straightforward to derive from the integral eigenproblem (2.13) the following estimate (see, e.g., [92, Thm 3.1]).

Theorem 4.1. *Let u be a c-bandlimited function given by* (4.5)*. Then we have*

$$\|\pi_N^c u-u\|\le \lambda_{N+1}\|\phi\|, \quad \forall c>0, \tag{4.6}$$

where λ_{N+1} is the eigenvalue in (2.13).

Note that $\lambda_N(c)$ decays super-geometrically (cf. [92, (2.17)]):

$$\lambda_N(c)\sim \exp\big(\tilde{N}(\kappa-\log\tilde{N})\big), \quad \kappa=\log\frac{ec}{4}, \quad \tilde{N}=N+\frac{1}{2}\gg 1. \tag{4.7}$$

Consequently, the PSWF with bandwidth parameter c provides an optimal approximation to the c-bandlimited functions.

4.2 Approximation results in Sobolev spaces

We now review the PSWF approximation of functions in general Sobolev spaces. The following estimates can be founded in [13, Thm. 3.1].

Theorem 4.2. *If*

$$r_{_N}:=\frac{c}{\sqrt{\chi_N}}<1, \tag{4.8}$$

then for any $u\in H^s(\Lambda)$ with integer $s\ge 0$, we have the bound for the expansion coefficient in (4.1)*:*

$$|\hat{u}_N(c)|\le C\big(N^{-\frac{2}{3}s}\|u\|_s+(r_{_N})^{\delta N}\|u\|\big), \tag{4.9}$$

where C and δ are positive constants independent of u, N and c.

Remark 4.1. Boyd [7] stated a similar result with the condition

$$r_N := \frac{c}{c_N^*} < 1 \quad \text{where} \quad c_N^* = \frac{\pi}{2}\Big(N+\frac{1}{2}\Big), \tag{4.10}$$

in place of (4.8).

It is apparent that for small fixed $c>0$, the PSWFs should have an approximability similar to the Legendre polynomials. However, we observe from (4.9) that $|\hat{u}_N| = O(N^{-2/3s})$, while the optimal order is expected to be $O(N^{-s})$. Wang and Zhang [95, Thm. 2.2] improved the above estimates in the following sense.

Theorem 4.3. *Let $c>0$, and $q_N = c/\sqrt{\chi_N}$. Given a positive constant $q_* < 1$, if*

$$q_N \le \frac{q_*}{\sqrt[6]{2}} \approx 0.8909 q_*, \tag{4.11}$$

and

$$u \in B^s(\Lambda) := \big\{u : (1-x^2)^{k/2}\partial_x^k u \in L^2(\Lambda), 0 \le k \le s\big\} \tag{4.12}$$

with integer $s \ge 0$, we have the estimate

$$|\hat{u}_N(c)| \le D\big(N^{-s}\|(1-x^2)^{s/2}\partial_x^s u\| + (q_*)^{\delta N}\|u\|\big), \tag{4.13}$$

where D and δ are positive constants independent of u, N and c.

As the second term in the upper bound of (4.13) is exponentially small for fixed $c>0$, we have optimal convergence rate $O(N^{-s})$. In (4.11), the feasible range of c is given explicitly in terms of $\chi_N(c)$, but it is more informative to understand c in terms of N. It is clear that from (2.31), we have

$$\frac{c}{\sqrt{N(N+1)+c^2}} < q_N < \frac{c}{N}, \tag{4.14}$$

so we infer from (4.11) that

$$c < c^*(N) := \frac{N}{\sqrt[6]{2}} \approx 0.8909 N. \tag{4.15}$$

Consequently, the PSWF approximation has a guaranteed spectral accuracy when one chooses $c \in (0, c^*(N))$. We refer to [95] for numerical justifications.

Using Theorem 4.3, one can obtain the following estimate of the L^2-projection error (see [96, Appendix B]).

Theorem 4.4. *Under the same conditions as in Theorem* 4.3, *we*

$$\|\pi_N^c u - u\| \le D\Big(N^{1/2-s}\big\|(1-x^2)^{s/2}\partial_x^s u\big\| + \frac{1}{\sqrt{\delta \ln(1/q_*)}}(q_*)^{\delta N}\|u\|\Big), \tag{4.16}$$

where D and δ are positive constants independent of u, N and c.

Remark 4.2. Wang [92] considered PSWF approximation in Sobolev spaces characterised by the Sturm-Liouville operator (2.19), where the bandwidth parameter was implicitly built in the norms. The analysis techniques in [13, 95] can be applied to the analysis of approximation by Mathieu functions for PDEs in elliptical geometry [80, 95].

5 Prolate spectral/spectral-element methods

In this section, we elaborate on the spectral and spectral-element methods using PSWFs as basis functions, and demonstrate the advantages over the polynomial-based methods when the underlying solutions are almost bandlimited and highly oscillatory.

5.1 Prolate-pseudospectral/collocation methods for hyperbolic PDEs

As already mentioned, an important motivation of using PSWFs as basis functions is to relax the CFL restriction of the time-stepping size of an explicit marching scheme e.g., the Runge-Kutta method. Indeed, the PSWFs oscillate nearly uniformly which lead to quasi-uniform grids, better conditioned pseudospectral differentiation matrices and better spatial resolution.

Chen *et al.* [13] considered the prolate-pseudospectral method for the one-way wave equation:

$$u_t - u_x = 0, \quad x \in (-1,1); \quad u(1,t) = g(t), \quad u(x,0) = f(x). \tag{5.1}$$

Let $\{x_j\}_{j=0}^N$ (arranged in ascending order) be the PL points and $\{h_j\}$ be the associated cardinal basis defined in (3.26). We seek the PSWF approximation of u in space:

$$u_N(x,t) = \sum_{j=0}^{N} u_N(x_j,t) h_j(x), \tag{5.2}$$

and find $\boldsymbol{u}(t) = (u_N(x_0,t), \cdots, u_N(x_N,t))^t$ via the penalty Galerkin method:

$$\boldsymbol{M}\frac{d\boldsymbol{u}}{dt} = \boldsymbol{S}\boldsymbol{u} - \tau(u_N(1,t) - g(t))\boldsymbol{e}_N, \ t > 0; \quad \boldsymbol{u}(0) = \boldsymbol{f}, \tag{5.3}$$

where $\tau > 0$ is a penalty constant, $\boldsymbol{e}_N$ is the unit vector with the last entry being 1, $\boldsymbol{f} = (f(x_0), \cdots, f(x_N))^t$, and the matrices $\boldsymbol{M}$ and $\boldsymbol{S}$ are

$$m_{ij} = \int_{-1}^{1} h_j(x) h_i(x) dx, \quad s_{ij} = \int_{-1}^{1} h_j'(x) h_i(x) dx. \tag{5.4}$$

It is shown in [13, Thm. 4.1] that the scheme (5.3) is stable if $\tau \geq 1/2$. In practice, over-integration is needed to evaluate the integrals in (5.4), so that the induced numerical errors are negligible. In [13], a 10th-order explicit Runge-Kutta method is adopted in time discretisation of (5.3), and the numerical results show that (i) the PSWF method

offers a systematic way of balancing accuracy and stability; and (ii) the choice of $c=N/2$ is suggested.

Note that one can use the prolate-collocation scheme to solve (5.1) with strong imposition of the boundary condition, that is, to find $u_N(\cdot,t)\in V_N^c$ for all $t>0$ such that

$$\begin{aligned}&\partial_t u_N(x_i,t)-\partial_x u_N(x_i,t)=0,\quad 0\le i\le N-1;\\&u_N(1,t)=g(t),\quad u_N(x_i,0)=f(x_i),\quad 0\le i\le N.\end{aligned}\tag{5.5}$$

Like (5.2), we can write

$$u_N(x,t)=\sum_{j=0}^{N-1}u_N(x_j,t)h_j(x)+g(t)h_N(x).\tag{5.6}$$

Inserting it into the scheme (5.5) leads to the system

$$\frac{d\bar{\boldsymbol{u}}}{dt}=\bar{\boldsymbol{D}}\bar{\boldsymbol{u}}+g(t)\boldsymbol{d},\ \ t>0;\quad \bar{\boldsymbol{u}}(0)=\bar{\boldsymbol{f}},\tag{5.7}$$

where $\bar{\boldsymbol{u}}$ and $\bar{\boldsymbol{f}}$ are column-N vectors by removing the last entry from $\boldsymbol{u}$ and $\boldsymbol{f}$ in (5.3), respectively, and

$$\boldsymbol{d}=(h_N'(x_0),\cdots,h_N'(x_{N-1}))^t,\quad \bar{\boldsymbol{D}}=(h_j'(x_i))_{0\le i,j\le N-1}.\tag{5.8}$$

In fact, Kovvali *et al.* [50] discussed the solution of (5.1) by using the alternative cardinal basis $\{l_j\}$ in (3.33), which allows for the prolate pseudospectral differentiation to be carried out in a rapid manner by using the fast multipole method. Kong and Rokhlin [47] applied a new differentiation scheme (see Subsection 3.6) to wave equations.

5.2 Prolate-pseudospectral/collocation methods for BVPs

To fix the idea, we consider the model equation:

$$\mathbb{L}[u](x):=u''(x)+p(x)u'(x)+q(x)u(x)=f(x),\quad x\in\Lambda;\quad u(\pm1)=u_\pm,\tag{5.9}$$

where p,q,f are continuous functions in Λ, and $u_\pm$ are given constants.

Let U_N^c be a generic finite dimensional space spanned by PSWF or PSWF-related basis functions, that is,

$$U_N^c:=\text{span}\{\beta_j:0\le j\le N\}.\tag{5.10}$$

Assume that

$$U_N^{0,c}:=H_0^1(\Lambda)\cap U_N^c=\text{span}\{\beta_j:1\le j\le N-1\}.\tag{5.11}$$

Like a typical polynomial approximation, the collocation scheme for (5.9) is to find $u_N\in U_N^c$ such that

$$u_N''(x_j)+p(x_j)u_N'(x_j)+q(x_j)u_N(x_j)=f(x_j),\ \ 1\le j\le N-1;\quad u_N(\pm1)=u_\pm.\tag{5.12}$$

We then consider the matrix form of the scheme under this generic basis:

$$u_N(x)=u_N^*(x)+\sum_{j=1}^{N-1}\tilde{u}_j\beta_j(x);\quad u_N^*(x)=\tilde{u}_0\beta_0(x)+\tilde{u}_N\beta_N(x), \tag{5.13}$$

where $\tilde{u}_0,\tilde{u}_N$ are uniquely determined by $u_N^*(\pm1)=u_\pm$. Inserting (5.13) into (5.12) leads to the linear system

$$\boldsymbol{A}\tilde{\boldsymbol{u}}=\boldsymbol{f},\quad \text{where } \boldsymbol{A}=\big(\mathbb{L}[\beta_j](x_i)\big)_{1\le i,j\le N-1}, \tag{5.14}$$

and $\boldsymbol{f}=\big(f(x_1)-\mathbb{L}[u_N^*](x_1),\cdots,f(x_{N-1})-\mathbb{L}[u_N^*](x_{N-1})\big)^t$. In practice, we have different choices of $\{\beta_j\}$ e.g., PSWF nodal basis and PSWF-related modal basis as reviewed previously and outlined below.

(i) Choose $\{\beta_j\}$ to be the PSWF cardinal basis: $\{h_j\}$ (cf. (3.26) or $\{l_j\}$ (cf. (3.33)). Ample numerical evidences show that with a suitable choice of c, the conditioning of the system (5.14) behaves like $O(N^3)$, as opposite to $O(N^4)$ in the Legendre case.

(ii) Choose $\{\beta_j\}$ to be $\{B_j\}$ in (3.36)-(3.38). In this case, the matrix of the highest derivative is identity, and the system (5.14) is well-conditioned (see [96]). Thanks to (3.35), one can also precondition the usual collocation scheme in (i) by the matrix $\boldsymbol{B}_{\text{in}}$ generated from $\{B_j\}$, and the resulted preconditioned system is well-conditioned (cf. [96]).

(iii) Choose $\{\beta_j\}$ to be $\{\phi_j\}$ in (3.59). As shown in [47], the condition number of the system (5.14) is about $O(N^2)$, but some effort is needed to compute the basis functions.

(iv) Choose $\{\beta_j\}$ to be the generalised PSWFs $\{q_j\}$ in (3.66). Thanks to (3.80), the conditioning of the system is $O(c^2)$.

One might also wish to employ the PSWF-pseudospectral method based on the Galerkin formulation with numerical integration. We consider the BVP in the self-adjoint form:

$$-(a(x)u'(x))'+b(x)u(x)=g(x),\quad x\in\Lambda;\quad u(\pm1)=0, \tag{5.15}$$

where $0<a_0<a(x)<a_1$. The PSWF-pseudospectral scheme for (5.15) is to find $u_N\in U_N^{0,c}$ such that

$$\langle au_N',v_N'\rangle_N+\langle bu_N,v_N\rangle_N=\langle g,v_N\rangle_N,\quad \forall v_N\in U_N^{0,c}, \tag{5.16}$$

where $\langle\cdot,\cdot\rangle_N$ is the discrete inner product related to a prolate-quadrature as described in Subsection 3.3. As commented in (3.18)-(3.19), it is hard to constructed a quadrature rule as good as the polynomial counterpart. However, one can use the generalized PSWFs of order -1 (cf. (3.66)) introduced in [106] as basis functions, and usual LGL quadrature with over-integration for variable coefficient problems.

Remark 5.1. Thanks to the relation between the mass and stiffness matrices in (3.82), we see that if $a=1$ and $b=c^2$ and under the Galerkin formulation with the continuous inner product in place of the discrete inner product, the coefficient matrix becomes diagonal. In other words, such a basis can diagonalise the Helmholtz operator: $u''+c^2u$ in the spirit of [79]. We refer to [106] for the details.

5.3 Prolate-collocation/Galerkin methods for eigenvalue problems

Consider the model eigen-problem:

$$\text{Find } (\mu,u) \text{ such that } u''(x)=\mu u(x), \quad x\in(-1,1); \quad u(\pm1)=0, \tag{5.17}$$

which admits the eigen-pairs (μ_k,u_k):

$$\mu_k=-\frac{k^2\pi^2}{4}, \quad u_k(x)=\sin\frac{k\pi(x+1)}{2}, \ k\geq 1. \tag{5.18}$$

The corresponding discrete eigen-problems are

$$\text{Find } (\tilde{\mu},\tilde{\boldsymbol{u}}) \text{ such that } \boldsymbol{D}_{\text{in}}^{(2)}\tilde{\boldsymbol{u}}=\tilde{\mu}\tilde{\boldsymbol{u}}; \quad \text{or} \quad \text{Find } (\hat{\mu},\hat{\boldsymbol{u}}) \text{ such that } \widehat{\boldsymbol{D}}_{\text{in}}^{(2)}\hat{\boldsymbol{u}}=\hat{\mu}\hat{\boldsymbol{u}}, \tag{5.19}$$

where $\boldsymbol{D}_{\text{in}}^{(2)}$ and $\widehat{\boldsymbol{D}}_{\text{in}}^{(2)}$ are defined in Subsection 3.4. We examine the relative errors:

$$\tilde{e}_j:=\frac{|\tilde{\mu}_j-\mu_j|}{|\mu_j|}, \quad \hat{e}_j:=\frac{|\hat{\mu}_j-\mu_j|}{|\mu_j|}, \quad 1\leq j\leq N-1.$$

In the computation, (c,N) is paired up by the approximate Kong-Rokhlin's rule with $\varepsilon=10^{-14}$. We plot in Figure 3 (quoted from [96]) the relative errors between the discrete and continuous eigenvalues of the prolate differentiation matrices with $c=120\pi$ and $N=284$, compared with those of the Legendre differentiation matrix at the LGL points. Among 283 eigenvalues of $\boldsymbol{D}_{\text{in}}^{(2)}$, 245 (approximately 87%) are accurate to at least 12 digits with respect to the exact eigenvalues, while only 72 (approximately 25%) of the Legendre case are of this accuracy. A very similar number of accurate eigenvalues is also obtained from $\widehat{\boldsymbol{D}}_{\text{in}}^{(2)}$.

We next apply the prolate-Galerkin method using the generalized PSWFs in Subsection 3.7:

$$\text{Find } (\breve{\mu},\breve{\boldsymbol{u}}) \text{ such that } \boldsymbol{S}\breve{\boldsymbol{u}}=\breve{\mu}\boldsymbol{M}\breve{\boldsymbol{u}} \text{ or } \widetilde{\boldsymbol{\Sigma}}\breve{\boldsymbol{u}}=(\breve{\mu}-c^2)\boldsymbol{M}\breve{\boldsymbol{u}}, \tag{5.20}$$

where the matrices are the same in (3.82). According to [98,108], there are about $2/\pi$ portion of "trusted" eigenvalues for the polynomial spectral method in 1D, where "trusted" means at least $O(N^{-1})$ accuracy. In Table 1, we tabulate the percentages of "trusted" discrete eigenvalues obtained by two methods for various (c,N). Observe again that the generalized PSWF method leads to a significant higher portion of "trusted" eigenvalues. Therefore, the generalized PSWFs have a better resolution of waves with fewer number of points per wavelength than polynomials.

DOI https://doi.org/10.4208/jms.v50n2.17.01 | Generated on 2024-11-19 16:37:05

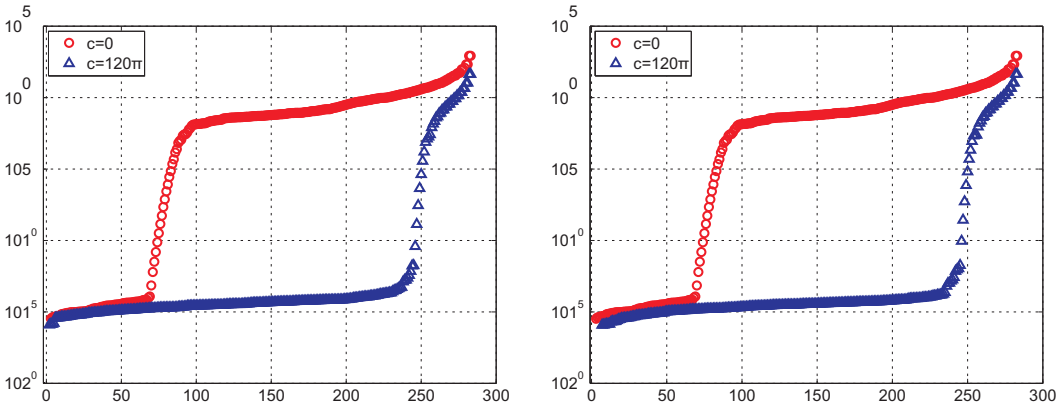

Figure 3: The relative errors $\{\tilde{e}_j\}_{j=1}^{N-1}$ (left) and $\{\hat{e}_j\}_{j=1}^{N-1}$ (right), obtained by $c=120\pi,\varepsilon=10^{-14}$ and $N=284$. The prolate differentiation matrices $\boldsymbol{D}_{\text{in}}^{(2)}$ (left, marked by "△") and $\widehat{\boldsymbol{D}}_{\text{in}}^{(2)}$ (right, marked by "△"), against the Legendre case (marked by "○").

Table 1: Comparison of percentage of "trusted" eigenvalues.

N	Generalized PSWFs		Legendre
	c	Percentage	Percentage$(\approx 2/\pi)$
67	20π	$52/67\approx 77.6\%$	$42/67\approx 62.7\%$
101	35π	$82/101\approx 81.1\%$	$62/98\approx 63.3\%$
454	200π	$417/454\approx 91.9\%$	$289/454\approx 63.6\%$
668	300π	$621/668\approx 93.0\%$	$425/668\approx 63.6\%$
882	400π	$825/882\approx 93.5\%$	$561/882\approx 63.6\%$
987	450π	$926/987\approx 93.8\%$	$628/987\approx 63.6\%$
1093	500π	$1028/1093\approx 94.0\%$	$696/1093\approx 63.6\%$
1307	600π	$1232/1307\approx 94.3\%$	$832/1307\approx 63.6\%$

5.4 Prolate-element methods and nonconvergence of h-refinement

Through simply examining hp-prolate approximation of the trivial function $u(x)\equiv 1$, Boyd *et al.* [10] demonstrated that in contrast to polynomials, such an approximation does not converge when the partition is refined but p. A justification was provided in Wang *et al.* [96]. To fix the idea, we consider the approximation of $u(x)$ defined on $\Omega:=(a,b)$ with a uniform partition:

$$\bar{\Omega}=\bigcup_{i=1}^{M}\bar{I}_i,\quad I_i:=(a_{i-1},a_i),\quad a_i=a+ih,\quad h=\frac{b-a}{M},\quad 1\le i\le M. \tag{5.21}$$

DOI https://doi.org/10.4208/jms.v50n2.17.01 | Generated on 2024-11-19 16:37:05

Note that the mapping between I_i and the reference interval $\Lambda:=(-1,1)$ is given by

$$x=\frac{h}{2}y+\frac{a_{i-1}+a_i}{2}=\frac{hy+2a+(2i-1)h}{2},\quad x\in I_i,\quad y\in\Lambda. \tag{5.22}$$

For any $u(x)$ defined in Ω, we denote

$$u|_{x\in I_i}=u^{I_i}(x)=\hat{u}^{I_i}(y),\quad x=\frac{hy+2a+(2i-1)h}{2}\in I_i,\quad y\in\Lambda. \tag{5.23}$$

We consider the hp-prolate approximation of u by

$$\big(\boldsymbol{\pi}^c_{h,N}u\big)\big|_{I_i}(x)=\sum_{n=0}^{N}\hat{u}^{I_i}_n(c)\psi_n(y;c)\quad\text{with}\quad\hat{u}^{I_i}_n(c)=\int_\Lambda\hat{u}^{I_i}(y)\psi_n(y;c)dy. \tag{5.24}$$

To describe the errors, we introduce the broken Sobolev space:

$$\widetilde{H}^\sigma(a,b)=\big\{u:u^{I_i}\in H^\sigma(I_i),1\le i\le M\big\},\ \sigma\ge1, \tag{5.25}$$

equipped with the norm and semi-norm

$$\|u\|_{\widetilde{H}^\sigma(a,b)}=\Big(\sum_{i=1}^{M}\|u^{I_i}\|^2_{H^\sigma(I_i)}\Big)^{\frac12},\quad |u|_{\widetilde{H}^\sigma(a,b)}=\Big(\sum_{i=1}^{M}\big\|\partial_x^\sigma u^{I_i}\big\|^2_{L^2(I_i)}\Big)^{\frac12}.$$

Theorem 5.1. [96, Thm 4.1]. *For any constant $q_*<1$, if*

$$\frac{c}{\sqrt{\chi_N}}\le\frac{q_*}{\sqrt[6]{2}}\approx0.8909q_*, \tag{5.26}$$

then for any $u\in\widetilde{H}^\sigma(a,b)$ with $\sigma\ge1$, we have

$$\|\boldsymbol{\pi}^c_{h,N}u-u\|_{L^2(a,b)}\le D\bigg\{\sqrt{N}\Big(\frac{h}{N}\Big)^\sigma|u|_{\widetilde{H}^\sigma(a,b)}+\frac{1}{\sqrt{\delta\ln(1/q_*)}}(q_*)^{\delta N}\|u\|_{L^2(a,b)}\bigg\}, \tag{5.27}$$

where D and δ are positive constants independent of u,N and c.

Observe from (5.27) that the second error term in the upper bound is independent of h. This implies that for fixed N, the refinement of h does not lead to any convergence in h, when the second term dominates the error. In view of this, it is advisable to use the p-version prolate-element method. It is noteworthy that the prolate-element method can be implemented as with the usual spectral-element method by swapping the basis and quadrature rules, while the choice of c can follow the rule in Subsection 3.2.

To demonstrate the performance of p-version prolate-element method, we revisit the Helmholtz equation in a heterogeneous medium considered in [96]:

$$\begin{aligned}&(c^2(x)u'(x))'+k^2n^2(x)u(x)=0,\quad x\in\Omega=(a,b);\\&u(a)=u_a,\quad(cu'-\mathrm{i}knu)(b)=0,\\&u,\,c^2u'\text{ are continuous on }\Omega,\end{aligned} \tag{5.28}$$

where the wavenumber $k>0$. Here, we take $\Omega=(0,1)$, $f(x)=1$ and consider the problem (5.28) with piecewise smooth coefficients:

$$c(x)=\begin{cases}1+x^2, & 0<x<0.25,\\ 1-x^2, & 0.25<x<0.5,\\ 1, & 0.5<x<1,\end{cases} \quad n(x)=\begin{cases}1.75+x, & 0<x<0.25,\\ 1.25-x, & 0.25<x<0.5,\\ 2, & 0.5<x<1.\end{cases}$$

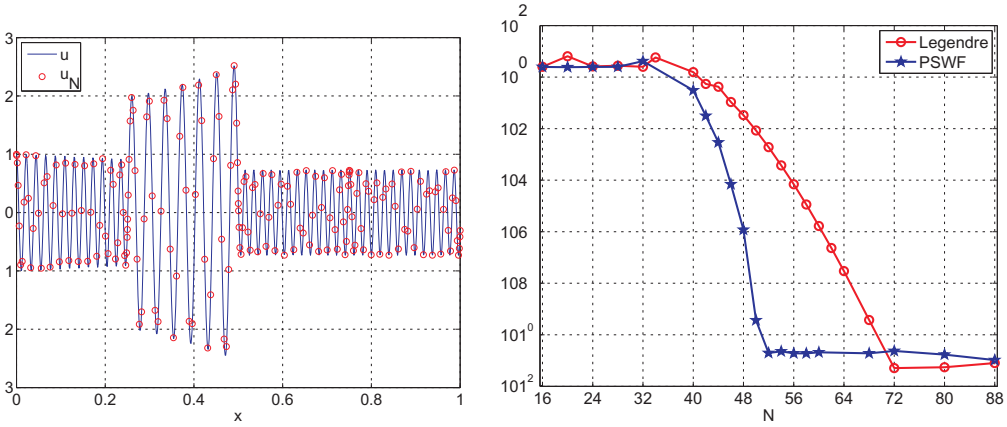

Figure 4: Real part (left) of the reference "exact" solution u computed by $(c,N)=(177,144)$ and $k=160$, against the numerical solution u_N of the prolate-element method with $(c,N)=(36,48)$. The maximum point-wise error is 1.19×10^{-6}. Right: Maximum point-wise errors of Legendre spectral-element and prolate-element methods.

We partition Ω into four subintervals of equal length, and compute a reference "exact" solution using very fine grids by the prolate-element method with $(c,N)=(177,144)$ (paired up by the Kong-Rokhlin's rule). In Figure 4 (left) (cf. [96]), we plot the real part of the "exact" solution with $k=160$ against the numerical solution obtained very coarse grids with $(c,N)=(36,48)$, which approximates the highly oscillatory solution with an accuracy about 10^{-6}. In Figure 4 (right) (cf. [96]), we make a comparison of the convergence with the polynomial spectral elements. Here, we sample $c\in[4,52]$, and observe much faster convergence rate for the prolate approach.

We next review the prolate-element method for PDEs on the sphere [107]. The gridding on the sphere is based on a projection of the prolate-points by using the cubed-sphere transform, which is free of singularity and leads to quasi-uniform grids. As result, the proposed prolate-element method can relax the time step size constraint of an explicit time-marching scheme, and increase the accuracy and enhance the resolution. Note that the cubed-sphere transform was introduced to overcome the pole singularity induced by the spherical transform (cf. [71,72]). The basic idea is to partition the sphere into six identical patches through a central projection of the faces of the inscribed cube

onto the spherical surface so that each of the six local coordinates is free of singularity. In Figure 5, we compare the distribution of the mapped LGL and prolate-points by the cubed-sphere transform, which shows that the latter is more uniformly distributed. Consider the conservative transport on the sphere governed by the continuity equation in flux form (cf. [63]):

$$\frac{\partial \Phi}{\partial t}+\mathrm{div}(\Phi \boldsymbol{V})=0 \quad \text{on } S\times(0,T]; \quad \Phi|_{t=0}=\Phi_0, \tag{5.29}$$

where Φ is the advection field and $\boldsymbol{V}=(u,v)^t$ is the given horizontal wind vector on the unit sphere S.

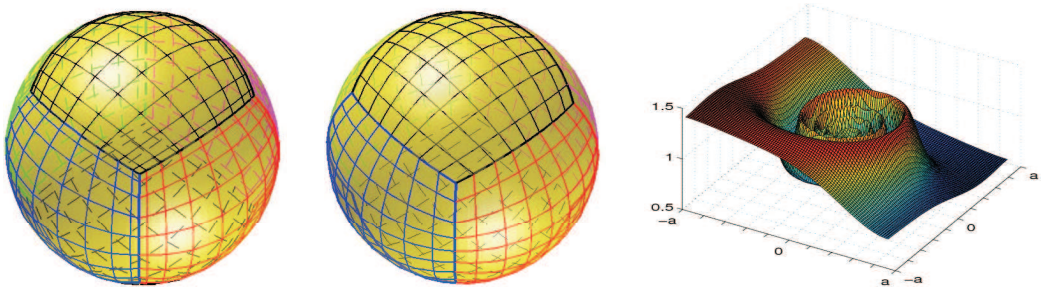

Figure 5: The grid distribution on the sphere with 10×10 points on each patch. Left: LGL points. Middle: prolate points with $c=8$. Right: Vortex near the north pole simulated by the prolate-element method with a third-order Adams-Bashforth time marching scheme.

We test the deformation flow (cf. [63]) consisting of two opposite vortices located at two poles as shown in Figure 5 (right). Indeed, we demonstrated in [107] that the prolate-element method with cubed-sphere partition led to accurate simulations of various nonlinear PDEs on the sphere.

6 Generalisations of prolate spheroidal wave functions

The extension and generalisation of Slepian's time-frequency concentration problems and/or Slepian's functions in different senses have attracted much attention. Slepian [83] extended the earlier works [52, 86] to multidimensional settings, and introduced a family of generalized PSWFs from the finite Fourier transform on a unit disk. Beylkin *et al.* [3] explored some interesting issues of bandlimited functions in a disk. Simons *et al.* [81] gave an up-to-date review of time-frequency and time-scale concentration problems on a sphere. We also refer to the recent works [21, 109] along this line. SenGupta *et al.* [75] considered the concentration problem over disjoint frequency intervals. Another very important inspiration of the Slepian's seminal papers is the investigation of differential operators that commute with appropriate integral operators, see for example, the insightful analysis by Grünbaum *et al.* [28–30]. Zayed [103] showed by using

the theory of reproducing-kernel Hilbert spaces that there are other systems possessing a double orthogonality as the Slepian functions, and in turn the Slepian functions turn out to be a lucky special case under this framework. The work [68] extended (2.13) to a finite fractional Fourier transform with applications to simultaneously time and band concentrating signals in optical systems. Below, we review several extensions most relevant to spectral methods.

6.1 Prolate spheroidal wave equation and generalised PSWFs

The eigenfunctions of the prolate spheroidal wave equation (PSWE)

$$\Big\{-\frac{1}{\cos\theta}\frac{d}{d\theta}\Big(\cos\theta\frac{d}{d\theta}\Big)+\frac{m^2}{\cos^2\theta}+c^2\sin^2\theta\Big\}y=\lambda(m;c)y,\quad \theta\in(-\pi/2,\pi/2), \tag{6.1}$$

are known as the (angular) prolate spheroidal functions, which arise in diverse areas such as the nuclear shell model, atomic and molecular physics, the study of light scattering in optics and theoretical cosmological models involving spheroidal geometry [1, 23, 24, 56, 64]. Here, the integer m is the zonal wavenumber and c is the "bandwidth" parameter. Using the transformation $x=\cos\theta$ leads to the alternative form

$$\frac{d}{dx}\Big\{(1-x^2)\frac{dv}{dx}\Big\}-\Big\{\frac{m^2}{1-x^2}+c^2x^2\Big\}v=-\lambda v,\quad x\in(-1,1). \tag{6.2}$$

It is noteworthy that Huang, Xiao and Boyd [39] proposed adaptive radial basis function and Hermite function pseudospectral methods for solving this eigen-problem for very large bandwidth parameter. Alıcı and Shen [2] introduced efficient pseudospectral methods for the PSWE with small and very large bandwidth parameters.

With a substitution, Wang and Zhang [94] defined the generalised PSWFs of order $\alpha>-1$. More precisely, letting $v(x)=(1-x^2)^{m/2}u(x)$, yields

$$(1-x^2)\frac{d^2u}{dx^2}-2(m+1)x\frac{du}{dx}+\big(\chi-c^2x^2\big)u=0,\quad c>0;\ \chi=\lambda-m(m+1),$$

which can be written as the self-adjoint form:

$$(1-x^2)^{-m}\frac{d}{dx}\Big\{(1-x^2)^{m+1}\frac{d}{dx}u(x)\Big\}+\big(\chi-c^2x^2\big)u(x)=0,\quad c>0,\ x\in(-1,1). \tag{6.3}$$

Allowing m to be any real number >-1, we introduced the generalized PSWFs as the eigenfunctions of the singular Sturm-Liouville problem:

$$-(1-x^2)^{-\alpha}\frac{d}{dx}\Big\{(1-x^2)^{\alpha+1}\frac{d}{dx}\psi_n^{(\alpha)}(x;c)\Big\}+c^2x^2\psi_n^{(\alpha)}(x;c)=\chi_n^{(\alpha)}(c)\psi_n^{(\alpha)}(x;c), \tag{6.4}$$

for $c>0,\alpha>-1$ and $n\geq 0$. If $\alpha=0$, it reduces to the PSWFs of order zero. We refer to (3.64)-(3.65) and [94] for many properties.

Karoui and Souabni [45] further generalised the PSWFs of order α to an orthogonal system with parameters $\alpha,\beta>-1$, defined as the eigenfunctions of

$$-\omega^{(-\alpha,-\beta)}\frac{d}{dx}\left\{\omega^{(\alpha+1,\beta+1)}\frac{d}{dx}\psi_n^{(\alpha,\beta)}\right\}+c^2x^2\psi_n^{(\alpha,\beta)}=\chi_n^{(\alpha,\beta)}\psi_n^{(\alpha,\beta)}, \tag{6.5}$$

where $\omega^{(a,b)}(x)=(1-x)^a(1+x)^b$ as before. They reduce to the Jacobi polynomials when $c=0$, and include the generalised PSWFs in [94] as special cases when $\alpha=\beta>-1$.

Note that if $\alpha=\beta$, the generalised PSWFs are both eigenfunctions of the compact integral operators:

$$\begin{aligned}
&\mathcal{F}_c^{(\alpha)}[\phi](x)=\int_{-1}^{1}e^{\mathrm{i}cxt}\phi(t)\omega_\alpha(t)dt,\quad \omega_\alpha(t)=(1-t^2)^\alpha;\\
&\mathcal{Q}_c^{(\alpha)}[\phi](x)=\frac{1}{2^\alpha\sqrt{2\pi}\Gamma(\alpha+1)}\left(\mathcal{F}_c^{(\alpha)}\right)^*\circ\mathcal{F}_c^{(\alpha)}[\phi](x)\\
&\qquad\qquad=\int_{-1}^{1}\frac{J_{\alpha+\frac{1}{2}}(c|t-x|)}{(c|t-x|)^{\alpha+\frac{1}{2}}}\phi(t)\omega_\alpha(t)dt,
\end{aligned} \tag{6.6}$$

where $J_{\alpha+\frac{1}{2}}(\cdot)$ is the Bessel function of the first kind. However, for the un-symmetric case $\alpha\neq\beta$, these attractive properties and important analytic tools appear not available. Using the notion of a restricted Paley-Wiener space, Karoui and Souabni [45] related $\{\psi_n^{(\alpha,\beta)}(x;c)\}$ to the solution of a generalised energy maximisation problem.

Motivated by Guo, Shen and Wang [31, 32], Zhang *et al.* [106] introduced a family of generalised PSWFs of order -1 for second-order BVPs (see Subsection 3.7 and Subsection 5.2). In fact, we can further define generalised PSWFs $\{\psi_n^{(-k,-l)}(x;c)\}$ with integers $k,l\geq 1$, by the reflecting property:

$$\psi_n^{(-k,-l)}(x;c)=(1-x)^k(1+x)^l\psi_{n-k-l}^{(k,l)}(x;c);\quad n\geq k+l, \tag{6.7}$$

which can serve as basis functions for higher-order BVPs with homogeneous Dirichlet boundary conditions.

Slepian [83] discussed the time-frequency concentration problem on a unit disk:

$$\gamma\psi(x,y)=\int_D e^{\mathrm{i}c(x\xi+y\eta)}\psi(\xi,\eta)d\xi d\eta,\quad c>0,$$

where $D=\{(x,y):x^2+y^2\leq 1\}$. This induces a family of circular PSWFs as the eigenfunctions of the integral operator:

$$\mu\phi(r)=\int_0^1 J_\alpha(crs)\sqrt{crs}\phi(s)ds,\quad 0\leq r\leq 1, \tag{6.8}$$

which is actually related to the finite Hankel transform (cf. [44]). As shown in [105], such a family is closely related to the Jacobi functions $\left\{x^{\alpha+1/2}P_n^{(\alpha,0)}(1-2x^2)\right\}$ for $x\in(-1,1)$

and $\alpha \geq -1/2$. In [104], we non-trivially extend prolate spheroidal wave functions on d-dimensional balls which are eigenfunctions of the finite Hankel transform, and also generalise the orthogonal polynomials on the balls (see, e.g., [16, 55]).

6.2 Oblate spheroidal wave functions

A spheroid, or ellipsoid of revolution, is a quadric surface obtained by rotating an ellipse about one of its principal axes; in other words, an ellipsoid with two equal semi-diameters. If the ellipse is rotated about its major axis, the result is a prolate (elongated) spheroid, like an American football or rugby ball. If the ellipse is rotated about its minor axis, the result is an oblate (flattened) spheroid, like a lentil.

The oblate spheroidal wave functions (OSWFs) are arisen from the separation of variables solving the Helmholtz problems in the oblate spheroidal geometry. With a change of $c \to \mathrm{i}c$ in (6.1)-(6.2), the eigenfunctions of the resulted eigen-problem are the corresponding OSWFs or their generalisations, denoted by $\phi_n(x;c)$,$\phi_n^{(\alpha)}(x;c)$ and $\phi_n^{(\alpha,\beta)}(x;c)$. In other words, we have $\phi_n(x;c) = \psi_n(x;\mathrm{i}c)$. Thanks to this relation, we can transplant the properties of the PSWFs to the OSWFs. For example, the OSWFs of order zero are eigenfunctions of both operators

$$\mathcal{L}_x^c[\phi] = \Big\{ \frac{d}{dx}(1-x^2)\frac{d}{dx} + c^2x^2 \Big\}\phi; \quad \mathcal{I}_x^c[\phi] = \int_{-1}^{1} e^{cxt}\phi(t)dt. \tag{6.9}$$

Indeed, they are commutable (cf. [103, Ex.5.2]). It is important to point out that in contrast with the PSWFs, the OSWFs become more oscillatory near the endpoints $x = \pm 1$, as c increases, which should be more suitable to be the basis functions for problems with boundary layers.

In [61], the generalised OSWFs were introduced as the eigenfunctions of the Sturm-Liouville problem:

$$-\omega^{(-\alpha,-\beta)}\frac{d}{dx}\Big\{\omega^{(\alpha+1,\beta+1)}\frac{d}{dx}\phi_n^{(\alpha,\beta)}\Big\} - \big\{c^2x^2 + cx(\beta-\alpha)\big\}\phi_n^{(\alpha,\beta)} = \chi_n^{(\alpha,\beta)}\phi_n^{(\alpha,\beta)}, \tag{6.10}$$

for $\alpha,\beta > -1$ and $c > 0$. With the linear term "$cx(\beta-\alpha)$", this new family is also eigenfunctions of the integral operators:

$$\mathcal{I}_{c,x}^{(\alpha,\beta)}[\phi] = \int_{-1}^{1} e^{c(xt-1)}\phi(t)\omega^{(\alpha,\beta)}(t)dt, \tag{6.11}$$

$$\mathcal{Q}_{c,x}^{(\alpha,\beta)}[\phi] = \big(\mathcal{I}_{c,x}^{(\alpha,\beta)}\big)^* \circ \mathcal{I}_{c,x}^{(\alpha,\beta)}[\phi] = \int_{-1}^{1} K_{\alpha,\beta}(x,t)\phi(t)\omega^{(\alpha,\beta)}(t)dt, \tag{6.12}$$

where

$$K_{\alpha,\beta}(x,t) = e^{-2c}\int_{-1}^{1} e^{c(x+t)z}\omega^{(\alpha,\beta)}(z)dz$$

can be expressed in terms of the Whittaker function. It is evident that one can define a new system of generalised PSWFs by changing $c \to ic$ in (6.10), so the analytic tools related to (6.11)-(6.12) are available for the case $\alpha \neq \beta$. If $\alpha = \beta$, the operators in (6.11)-(6.12) with $c \to ic$ certainly reduce to the operators in (6.6).

7 Concluding remarks

Over the past fifteen years, there has been much renewed interest in the prolate spheroidal wave functions and related problems. It is not possible to provide a very comprehensive review of the developments in many subjects. It also appears ambitious to highlight and summarise the results on numerical analysis and computations using PSWFs and their variants. We therefore strive to focus on their applications in spectral and spectral-element methods for problems with oscillatory and almost bandlimited solutions. We emphasise the care needed to construct efficient spectral algorithms in comparison with polynomial-based approaches.

Acknowledgments

The research of the author is partially supported by Singapore MOE AcRF Tier 1 Grant (RG 27/15), and MOE AcRF Tier 2 Grant (MOE 2013-T2-1-095, ARC 44/13).

The author would like to thank the collaborators: Huiyuan Li, Zhijian Rong, Jie Shen, Jing Zhang and Zhimin Zhang, for their contributions to the works on this topic.

References

[1] M. Abramowitz, I. Stegun. Handbook of Mathematical Functions. Dover, New York, 1964.
[2] H. Alıcı, J. Shen. Highly accurate pseudospectral approximations of the prolate spheroidal wave equation for any bandwidth parameter and zonal wavenumber. J. Sci. Comput., DOI 10.1007/s10915-016-0321-7, 2016.
[3] G. Beylkin, C. Kurcz, L. Monzón. Grids and transforms for band-limited functions in a disk. Inverse Problems, 2007, 23(5):2059–2088.
[4] G. Beylkin, L. Monzón. On generalized Gaussian quadratures for exponentials and their applications. Appl. Comput. Harmon. Anal., 2002, 12(3):332–373.
[5] G. Beylkin, K. Sandberg. Wave propagation using bases for bandlimited functions. Wave Motion, 2005, 41(3):263–291.
[6] J.P. Boyd. Large mode number eigenvalues of the prolate spheroidal differential equation. Appl. Math. Comput., 2003, 145(2-3):881–886.
[7] J.P. Boyd. Prolate spheroidal wavefunctions as an alternative to Chebyshev and Legendre polynomials for spectral element and pseudospectral algorithms. J. Comput. Phys., 2004, 199(2):688–716.
[8] J.P. Boyd. Algorithm 840: computation of grid points, quadrature weights and derivatives for spectral element methods using prolate spheroidal wave functions—prolate elements. ACM Trans. Math. Software, 2005, 31(1):149–165.

[9] J.P. Boyd. Duration and bandwidth limiting: prolate functions, sampling, and applications [book review of MR2883827]. SIAM Rev., 2013, 55(3):574–575.
[10] J.P. Boyd, G. Gassner, B.A. Sadiq. The nonconvergence of h-refinement in prolate elements. J. Sci. Comput., 2013, 57(2):372–389.
[11] C. Canuto, M.Y. Hussaini, A. Quarteroni, T.A. Zang. Spectral Methods. Scientific Computation. Springer-Verlag, Berlin, Fundamentals in single domains, 2006.
[12] C.Y. Chen, P.P. Vaidyanathan. MIMO radar space-time adaptive processing using prolate spheroidal wave functions. IEEE Trans. Signal Process., 2008, 56(2):623–635.
[13] Q.Y. Chen, D. Gottlieb, J. Hesthaven. Spectral methods based on prolate spheroidal wave functions for hyperbolic PDEs. SIAM J. Numer. Anal., 2005, 43(5):1912–1933 (electronic).
[14] R. Courant, D. Hilbert. Methods of Mathematical Physics. Interscience Publishers, 1953, 1.
[15] D. Dąbrowska. Recovering signals from inner products involving prolate spheroidals in the presence of jitter. Math. Comp., 2005, 74(249):279–290 (electronic).
[16] F. Dai, Y. Xu. Approximation Theory and Harmonic Analysis on Spheres and Balls. Springer Monographs in Mathematics, Springer, New York, 2013.
[17] R.S. Dilmaghani, M. Ghavami, B. Allen, H. Aghvami. Novel UWB pulse shaping using prolate spheroidal wave functions. In Personal, Indoor and Mobile Radio Communications, 2003. PIMRC 2003. 14th IEEE Proceedings on, IEEE, 2003, 1: 602–606 .
[18] J. Duoandikoetxea. Fourier Analysis. Grad. Stud. Math., American Mathematical Society, Providence, RI, 2001, 29.
[19] M.E. Elbarbary. Integration preconditioning matrix for ultraspherical pseudospectral operators. SIAM J. Sci. Comput., 2006, 28(3):1186–1201 (electronic).
[20] W. Erb. An orthogonal polynomial analogue of the Landau-Pollak-Slepian time-frequency analysis. J. Approx. Theory, 2013, 166:56–77.
[21] W. Erb, S. Mathias. An alternative to Slepian functions on the unit sphere—a space-frequency analysis based on localized spherical polynomials. Appl. Comput. Harmon. Anal., 2015, 38(2):222–241.
[22] A. Erdélyi, W. Magnus, F. Oberhettinger, F. G. Tricomi. Higher Transcendental Functions. Vols. I, II. McGraw-Hill Book Company, Inc., New York-Toronto-London, 1953. Based, in part, on notes left by Harry Bateman.
[23] P.E. Falloon, P.C. Abbott, J.B. Wang. Theory and computation of spheroidal wave functions. J. Phys. A. Math. Theor., 2003, 36(20):5477.
[24] C. Flammer. Spheroidal Wave Functions. Stanford University Press, Stanford, CA, 1957.
[25] A. Glaser, X. Liu, V. Rokhlin. A fast algorithm for the calculation of the roots of special functions. SIAM J. Sci. Comput., 2007, 29(4):1420–1438.
[26] L. Gosse. Effective band-limited extrapolation relying on Slepian series and ℓ^1 regularization. Comput. Math. Appl., 2010, 60(5):1259–1279.
[27] L. Gosse. Compressed sensing with preconditioning for sparse recovery with subsampled matrices of Slepian prolate functions. ANNALI DELL'UNIVERSITA'DI FERRARA, 2013, 59(1):81–116.
[28] F.A. Grünbaum. Differential operators commuting with convolution integral operators. J. Math. Anal. Appl., 1983, 91(1):80–93.
[29] F.A. Grünbaum, L. Longhi, M. Perlstadt. Differential operators commuting with finite convolution integral operators: some non-abelian examples. SIAM J. Appl. Math., 1982, 42(5):941–955.
[30] F.A. Grünbaum, L. Miranian. Magic of the prolate spheroidal functions in various setups. In Proceedings of SPIE, 2001, 4478, page 151.

[31] B.Y. Guo, J. Shen, L.L. Wang. Optimal spectral-Galerkin methods using generalized Jacobi polynomials. J. Sci. Comput., 2006, 27(1-3):305–322.
[32] B.Y. Guo, J. Shen, L.L. Wang. Generalized Jacobi polynomials/functions and their applications. Appl. Numer. Math., 2009, 59(5):1011–1028 .
[33] Y. He, P.J. Li, J. Shen. A new spectral method for numerical solution of the unbounded rough surface scattering problem. J. Comput. Phys., 2014, 275:608–625.
[34] J. Hesthaven. Integration preconditioning of pseudospectral operators. I. Basic linear operators. SIAM J. Numer. Anal., 1998, 35(4):1571–1593.
[35] J.A. Hogan, S. Izu, J.D. Lakey. Sampling approximations for time- and bandlimiting. Sampl. Theory Signal Image Process., 2010, 9(1-3):91–117.
[36] J.A. Hogan, J.D. Lakey. Duration and Bandwidth Limiting. Applied and Numerical Harmonic Analysis, Birkhäuser/Springer, New York, 2012. Prolate Functions, Sampling, and Applications.
[37] J.A. Hogan, J.D. Lakey. Frame properties of shifts of prolate spheroidal wave functions. Appl. Comput. Harmon. Anal., 2015, 39(1):21–32.
[38] N. Hu, X. Xu, Z. Ye. DOA estimation for wideband signals based on sparse signal reconstruction using prolate spheroidal wave functions. Signal Processing, 2014, 96, Part B:395–400, .
[39] Z. Huang, J. Xiao, J.P. Boyd. Adaptive radial basis function and Hermite function pseudospectral methods for computing eigenvalues of the prolate spheroidal wave equation for very large bandwidth parameter. J. Comput. Phys., 2015, 281:269–284.
[40] A. Karoui. Uncertainty principles, prolate spheroidal wave functions, and applications. In Recent Developments in Fractals and Related Fields, Appl. Numer. Harmon. Anal., Birkhäuser Boston, Inc., Boston, MA, 2010, 165–190.
[41] A. Karoui. Unidimensional and bidimensional prolate spheroidal wave functions and applications. J. Franklin Inst., 2011, 348(7):1668–1694.
[42] A. Karoui, I. Mehrzi. Asymptotic behaviors and numerical computations of the eigenfunctions and eigenvalues associated with the classical and circular prolate spheroidal wave functions. Appl. Math. Comput., 2012, 218(22):10871–10888.
[43] A. Karoui, T. Moumni. New efficient methods of computing the prolate spheroidal wave functions and their corresponding eigenvalues. Appl. Comput. Harmon. Anal., 2008, 24:269–289.
[44] A. Karoui, T. Moumni. Spectral analysis of the finite Hankel transform and circular prolate spheroidal wave functions. J. Comput. Appl. Math., 2009, 233(2):315–333.
[45] A. Karoui, A. Souabni. Generalized prolate spheroidal wave functions: Spectral analysis and approximation of almost band-limited functions. J. Fourier Anal. Appl, 2016(22):383–412.
[46] K. Khare, N. George. Sampling theory approach to prolate spheroidal wavefunctions. J. Phys. A, 2003, 36(39):10011–10021.
[47] W.Y. Kong, V. Rokhlin. A new class of highly accurate differentiation schemes based on the prolate spheroidal wave functions. Appl. Comput. Harmon. Anal., 2012, 33(2):226–260.
[48] D. Kosloff, H. Tal-Ezer. A modified Chebyshev pseudospectral method with an $O(N^{-1})$ time step restriction. J. Comput. Phys., 1993, 104(2):457–469.
[49] K. Kou, J. Morais, Y. Zhang. Generalized prolate spheroidal wave functions for offset linear canonical transform in Clifford analysis. Math. Methods Appl. Sci., 2013, 36(9):1028–1041.
[50] N. Kovvali, W. Lin, L. Carin. Pseudospectral method based on prolate spheroidal wave functions for frequency-domain electromagnetic simulations. IEEE Trans. Antennas and

Propagation, 2005, 53:3990–4000.
[51] N. Kovvali, W. Lin, Z. Zhao, L. Couchman, L. Carin. Rapid prolate pseudospectral differentiation and interpolation with the fast multipole method. SIAM J. Sci. Comput., 2006, 28(2):485–497 (electronic).
[52] H.J. Landau, H.O. Pollak. Prolate spheroidal wave functions, Fourier analysis and uncertainty. II. Bell System Tech. J., 1961, 40:65–84.
[53] H.J. Landau, H.O. Pollak. Prolate spheroidal wave functions, Fourier analysis and uncertainty. III. The dimension of the space of essentially time- and band-limited signals. Bell System Tech. J., 1962, 41:1295–1336.
[54] B.H. Li. Hermite expansion of the Riemann Zeta function. J. Math. Study, 2016, 49(4):319–324.
[55] H.Y. Li, Y. Xu. Spectral approximation on the unit ball. SIAM J. Numer. Anal., 2014, 52(6):2647–2675.
[56] L.W. Li, X.K. Kang, M.S. Leong. Spheroidal Wave Functions in Electromagnetic Theory, John Wiley & Sons, 2004, 166.
[57] M.A. Lindquist, T.D. Wager. Spatial smoothing in fMRI using prolate spheroidal wave functions. Human Brain Mapping, 2008, 29(11):1276–1287.
[58] J.W. Miles. Asymptotic approximations for prolate spheroidal wave functions. Studies in Appl. Math., 1975, 54(4):315–349.
[59] L. Miranian. Slepian functions on the sphere, generalized Gaussian quadrature rule. Inverse Problems, 2004, 20(3):877–892.
[60] I.C. Moore, M. Cada. Prolate spheroidal wave functions, an introduction to the Slepian series and its properties. Appl. Comput. Harmon. Anal., 2004, 16(3):208–230.
[61] T. Moumni, A. Amara. On the generalized oblate spheroidal wave functions and applications. arXiv preprint arXiv:1410.3568, 2014.
[62] T. Moumni, A.I. Zayed. A generalization of the prolate spheroidal wave functions with applications to sampling. Integral Transforms Spec. Funct., 2014, 25(6):433–447.
[63] R.D. Nair, S.J. Thomas, R.D. Loft. A discontinuous Galerkin transport scheme on the cubed sphere. Mon. Weather Rev., 2005, 133(4):814–828.
[64] F.W.J. Olver, D.W. Lozier, R.F. Boisvert, C.W. Clark (Eds.). NIST Handbook of Mathematical Functions. Cambridge University Press, New York, 2010.
[65] A. Osipov, V. Rokhlin. On the evaluation of prolate spheroidal wave functions and associated quadrature rules. Appl. Comput. Harmon. Anal., 2014, 36(1):108–142.
[66] A. Osipov, V. Rokhlin, H. Xiao. Prolate Spheroidal Wave Functions of Order Zero. Series in Applied Mathematical Sciences Springer, 2013, 187.
[67] R. Paley, N. Wiener. Fourier Transforms in the Complex Domain. American Mathematical Society Colloquium Publications, American Mathematical Society, Providence, RI, 1987, 19. Reprint of the 1934 original.
[68] S.C. Pei, J.J. Ding. Generalized prolate spheroidal wave functions for optical finite fractional Fourier and linear canonical transforms. J. Opt. Soc. Amer. A, 2005, 22(3):460–474.
[69] A. Plattner, F.J. Simons. Spatiospectral concentration of vector fields on a sphere. Appl. Comput. Harmon. Anal., 2014, 36(1):1–22.
[70] V. Rokhlin, H. Xiao. Approximate formulae for certain prolate spheroidal wave functions valid for large values of both order and band-limit. Appl. Comput. Harmon. Anal., 2007, 22(1):105–123.
[71] C. Ronchi, R. Iacono, P.S. Paolucci. The "cubed sphere": a new method for the solution of partial differential equations in spherical geometry. J. Comput. Phys., 1996, 124(1):93–114.

[72] R. Sadourny. Conservative finite-difference approximations of the primitive equations on quasi-uniform spherical grids. Mon. Weather Rev., 1972, 100(2):136–144.
[73] S. Schmutzhard, T. Hrycak, H.G. Feichtinger. A numerical study of the Legendre-Galerkin method for the evaluation of the prolate spheroidal wave functions. Numer. Algorithms, 2015, 68(4):691–710.
[74] S. Senay, L.F. Chaparro, L. Durak. Reconstruction of nonuniformly sampled time-limited signals using prolate spheroidal wave functions. Signal Processing, 2009, 89(12):2585–2595.
[75] I. SenGupta, B. Sun, W. Jiang, G. Chen, M.C. Mariani. Concentration problems for bandpass filters in communication theory over disjoint frequency intervals and numerical solutions. J. Fourier Anal. Appl., 2012, 18(1):182–210.
[76] J. Shen. Efficient spectral-Galerkin method I. direct solvers for second- and fourth-order equations by using Legendre polynomials. SIAM J. Sci. Comput., 1994, 15:1489–1505.
[77] J. Shen, T. Tang, L.L. Wang. Spectral Methods: Algorithms, Analysis and Applications. Series in Computational Mathematics, Springer-Verlag, Berlin, Heidelberg, 2011, 41.
[78] J. Shen, L.L. Wang. Error analysis for mapped Legendre spectral and pseudospectral methods. SIAM J. Numer. Anal., 2005, 42(1):326–349.
[79] J. Shen, L.L. Wang. Fourierization of the Legendre-Galerkin method and a new space-time spectral method. Appl. Numer. Math., 2007, 57(5-7):710–720.
[80] J. Shen, L.L. Wang. On spectral approximations in elliptical geometries using Mathieu functions. Math. Comp., 2009, 78(266):815–844.
[81] F.J. Simons, F.A. Dahlen, M.A. Wieczorek. Spatiospectral concentration on a sphere. SIAM Rev., 2006, 48(3):504–536(electronic).
[82] F.J. Simons, D.V. Wang. Spatiospectral concentration in the Cartesian plane. GEM Int. J. Geomath., 2011, 2(1):1–36.
[83] D. Slepian. Prolate spheroidal wave functions, Fourier analysis and uncertainity. IV. Extensions to many dimensions; generalized prolate spheroidal functions. Bell System Tech. J., 1964, 43:3009–3057.
[84] D. Slepian. Some asymptotic expansions for prolate spheroidal wave functions. J. Math. and Phys., 1965, 44:99–140.
[85] D. Slepian. Some comments on Fourier analysis, uncertainty and modeling. SIAM Rev., 1983, 25(3):379–393.
[86] D. Slepian, H.O. Pollak. Prolate spheroidal wave functions, Fourier analysis and uncertainty. I. Bell System Tech. J., 1961, 40:43–63.
[87] G. Szegö. Orthogonal Polynomials (fourth edition). AMS Coll. Publ., 1975, 23.
[88] M. Taylor, B.A. Wingate. A generalization of prolate spheroidal functions with more uniform resolution to the triangle. J. Engrg. Math., 2006, 56(3):221–235.
[89] G. Walter. Prolate spheroidal wavelets: translation, convolution, and differentiation made easy. J. Fourier Anal. Appl., 2005, 11(1):73–84.
[90] G. Walter, X.P. Shen. Wavelets based on prolate spheroidal wave functions. J. Fourier Anal. Appl., 2004, 10(1):1–26.
[91] G. Walter, T. Soleski. A new friendly method of computing prolate spheroidal wave functions and wavelets. Appl. Comput. Harmon. Anal., 2005, 19(3):432–443.
[92] L.L. Wang. Analysis of spectral approximations using prolate spheroidal wave functions. Math. Comp., 2010, 79(270):807–827.
[93] L.L. Wang, M. Samson, X.D. Zhao. A well-conditioned collocation method using a pseudospectral integration matrix. SIAM J. Sci. Comput., 2014, 36(3):A907–A929.
[94] L.L. Wang, J. Zhang. A new generalization of the PSWFs with applications to spectral

approximations on quasi-uniform grids. Appl. Comput. Harmon. Anal., 2010, 29(3):303–329.
[95] L.L. Wang, J. Zhang. An improved estimate of PSWF approximation and approximation by Mathieu functions. J. Math. Anal. Appl., 2011, 379(1):35–47.
[96] L.L. Wang, J. Zhang, Z. Zhang. On hp-convergence of prolate spheroidal wave functions and a new well-conditioned prolate-collocation scheme. J. Comput. Phys., 2014, 268:377–398.
[97] G.N. Watson. A Treatise on the Theory of Bessel Functions. Cambridge University Press, 1966.
[98] J.A.C. Weideman, L.N. Trefethen. The eigenvalues of second-order spectral differentiation matrices. SIAM J. Numer. Anal., 1988, 25(6):1279–1298.
[99] H. Xiao. Prolate spheroidal wave functions, quadrature, interpolation, and asymptotic formulae. PhD Thesis, Yale University, 2001.
[100] H. Xiao, V. Rokhlin. High-frequency asymptotic expansions for certain prolate spheroidal wave functions. J. Fourier Anal. Appl., 2003, 9(6):575–596.
[101] H. Xiao, V. Rokhlin, N. Yarvin. Prolate spheroidal wavefunctions, quadrature and interpolation. Inverse Problems, 2001, 17(4):805–838. Special issue to celebrate Pierre Sabatier's 65th birthday (Montpellier, 2000).
[102] A.I. Zayed. Advances in Shannon's Sampling Theory. CRC Press, Boca Raton, FL, 1993.
[103] A.I. Zayed. A generalization of the prolate spheroidal wave functions. Proc. Amer. Math. Soc., 2007, 135(7):2193–2203(electronic).
[104] J. Zhang, H.Y. Li, L.L. Wang, Z. Zhang. Prolate spheroidal wave functions and finite Hankel transform on d-dimensional balls. In preparation, 2017.
[105] J. Zhang, L.L. Wang. On spectral approximations by generalized Slepian functions. Numer. Math. Theory Methods Appl., 2011, 4(2):296–318.
[106] J. Zhang, L.L. Wang, H.Y. Li, Z. Zhang. Optimal spectral schemes based on generalized prolate spheroidal wave functions of order -1. J. Sci. Comput., 2017, 70:451–477.
[107] J. Zhang, L.L. Wang, Z.J. Rong. Spectral-element methods on quasi-uniform grids for nonlinear PDEs on a sphere. J. Sci. Comput., 2011, 47(1):73–92.
[108] Z. Zhang. How many numerical eigenvalues can we trust? J. Sci. Comput., 2015, 65(2):455–466.
[109] K. Zubair, A.K. Rodney, D.M. Jason. Slepian spatial-spectral concentration on the ball. Appl. Comput. Harmon. Anal., 2016, 40(3):470–504.